AD-A064 214 AIR FORCE INST OF TECH WRIGHT-PATTERSON AFB OHIO SCH--ETC F/G 20/5
ANALYSIS OF AN INJECTION-LOCKED DYE RING LASER AMPLIFIER.(U)
DEC 78 J C VETTER

UNCLASSIFIED AFIT/GEP/PH/78D-15 NL

| OF |
AD
A064214

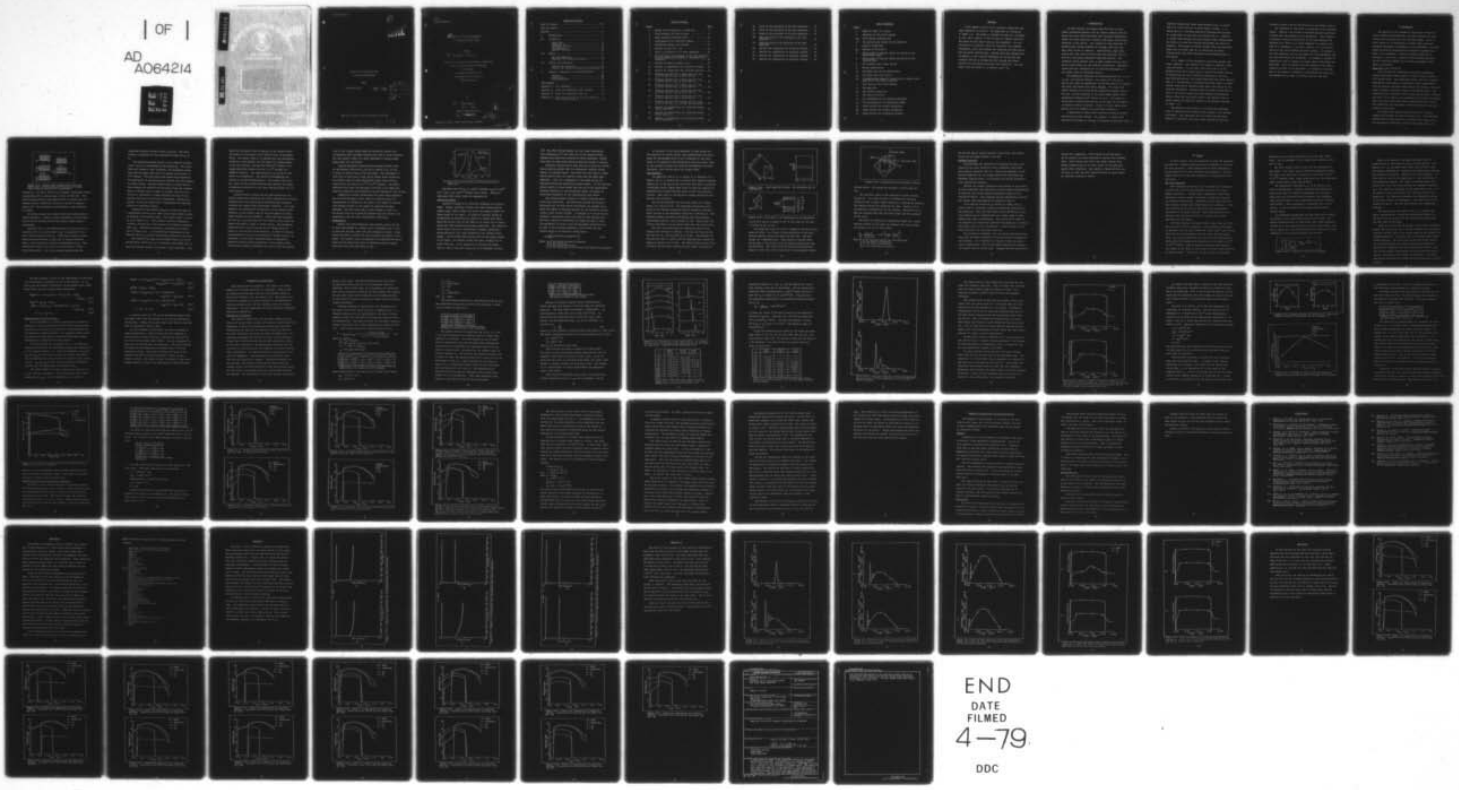

END
DATE
FILMED
4-79
DDC

AFIT/GEP/PH/78D-15

(1)

LEVEL II

ANALYSIS OF AN INJECTION-LOCKED DYE RING LASER AMPLIFIER

THESIS

AFIT/GEP/PH/78D-15

James C. Vetter
2nd Lt USAF

Approved for public release; distribution unlimited.

(14) AFIT/GEP/PH/78D-15

(6) ANALYSIS OF AN INJECTION-LOCKED DYE RING LASER AMPLIFIER

THESIS

(9) Master's thesis,

Presented to the Faculty of the School of Engineering

of the Air Force Institute of Technology

Air University

in Partial Fulfillment of the

Requirements for the Degree of

Master of Science

by

(10) James C. Vetter

2nd Lt USAF

Graduate Engineering Physics

(11) December 1978

(12) 76 p.

Approved for public release; distribution unlimited.

012225

Table of Contents

List of Figures

List of Symbols

Symbol	
c	Speed of light in a vacuum
D	Thickness of the active medium
K_{st}	Inter system crossing rate
L	The optical path length of the resonator
n	index of refraction
N_n	Density of the state n
p	Total number of photons within the cavity in the spontaneous modes
q	Total number of photons within the cavity at the injected mode
Q	The Q factor for a laser cavity
R	Mirror reflectivity
t_c	The decay time of the laser cavity
t_n	The decay time from level n
T_i	A dimensionless quantity accounting for losses other than due to the output coupling
v	The Volume of the active medium
W	The pump rate
W_c	The critical pump rate
η	The laser efficiency
λ_i	The wavelength of the injected radiation
λ_l	The wavelengths of the spontaneous modes
σ_a	Cross section for singlet absorption
σ_T	Cross section for triplet absorption
σ_f	Cross section for stimulated emission

Abstract

A rate equation model for an injection locked dye ring laser amplifier is derived. The amplifier is a design by A. Pease *et al*. The model is compared to work by G. Marowsky, C. Lin, and U. Ganiel *et al* and is shown to compare very well. The model is then used to analyze the amplifier. The conditions of the amplifier that are varied are the injected wavelength, delay time between the injection and pump pulses, and the mirror reflectivity. Results show that reabsorption of photons at the injected wavelength by the dye has significant effects on locking and that varying the mirror reflectivity partially alleviates this situation. The best delay times are found to be between 3 and 7 ns.

I Introduction

In 1966, Sorokin and Lankard were the first to ever obtain stimulated emission from an organic compound (Ref 14). Since that time, many researchers have devoted considerable effort to obtain efficient, tunable, high power, narrow band operation in dye lasers. Such lasers are very important in spectroscopy, isotope separation, biology, medicine, and many other fields of research. Unfortunately, high output powers have been achieved with broad band operation but not with the very narrow bandwidths sometimes desired. The classical tuning methods used in these efforts work by introducing heavy losses for the unwanted wavelengths. Substantial losses are also introduced for the desired wavelengths and the output power is decreased severly.

An alternative technique for achieving narrow band oscillation is injection locking. The output of a low power, narrow band laser is passed down the optical path of an untuned dye laser just before and during pumping. The input beam passes through the dye and causes stimulated emission out of the dye. As the intensity of the input signal grows, fewer spontaneous emissions are allowed to occur. The output is forced into a narrow band and the output power is the same as it would be without injection. There is still a broad background but it is usually of a very small intensity.

A great deal is known about injection locking in pulsed and continious wave systems. For example, R. Adler first analyzed the problem of locking in classical oscillators (Ref 1).

Injection locking was shown experimentally by H. L. Stover and W. H. Steir (Ref 15) in He-Ne lasers in 1966. C. J. Buczek and R. J. Freiberg described frequency stabilization in a high power cw CO_2 laser by locking (Ref 3). Interest in pulsed laser systems has grown because wider tuning ranges are obtained since free running wavelengths are easier to suppress. Many papers on pulsed systems have been published which help to reveal some of the conditions for which locking occurs and these conditions are discussed later in this paper.

A. A. Pease *et al* have designed an injection locked ring laser amplifier. The amplifier is simply an injection tuned ring oscillator. It is a cube with a slit cut in it for passing a dye, and a prism which is used as an output coupler by frustrating the total internal reflection of the cube. High efficiencies and very narrow bandwidths have been obtained from it. The amplifier is designed such that, when injection locked, there are no standing waves within the cavity at the injected wavelength. Although there has been a great deal of work in the area of using injection locking for tuning dye lasers, there has been little work in the specific area of using locking for amplifier systems of the kind as designed by Pease *et al*.

The purpose of this paper is to develop an analytical model to describe this amplifier and to apply it for varying conditions. The conditions that are varied are the wavelengths of injection, the delay times between the pump and

injection pulses, and the reflectivity of the output coupler.

The remainder of this paper is organized in the following manner. Chapter 2 is devoted to reviewing general properties of laser dyes and Rhodamine 6G in particular. Also, chapter 2 contains a detailed description of the ring amplifier as designed by A. Pease *et al*, brief summaries of relevant work done by G. Marowsky, C. Lin and U. Ganiel *et al*, and a brief review of the theory behind injection locking. In chapter 3, the rate equations used in this paper and the assumptions used for their derivation are presented. In chapter 4, results of computations used to support the model used in this paper are presented. Also in chapter 4 are the results of the computational analysis of the amplifier. In chapter 5, the work done in this paper is summarized, conclusions are drawn, and recommendations are made for further work in this area.

II Background

The purpose of this chapter is to provide a brief outline of organic dye properties, injection locking, the amplifier under consideration, and relevant papers. First, a brief review of the properties of organic laser dyes and important parameters of Rhodamine 6G are presented. Injection theory is briefly reviewed and the amplifier designed by A. Pease *et al* is presented. Finally, relevant papers by G. Marowsky, C. Lin, and U. Ganiel *et al* are outlined and their use for providing support for the model developed in this paper is discussed.

Laser Dyes (Ref 13:1375-6)

Dye molecules are complicated structures containing several conjugated double bonds (two double bonds separated by a single bond). This complexity causes the dye to contain hundreds of vibrational and rotational levels superimposed over the singlet (electron spins opposed) and triplet (electron spins alligned) electronic levels of its double bonds. The vibrational and rotational levels cause dye molecules to absorb and emit in broad bands; not necessarily at visible wavelengths. Most laser dyes absorb and emit at wavelengths above 200 nm. The vibrational and rotational levels are refered to as manifolds in this paper.

An energy level diagram characteristic of a typical organic dye molecule is shown in figure II-1. The electronic ground state of the molecule is a singlet state shown as N_1. The vibrational-rotational manifold associated with N_1 is

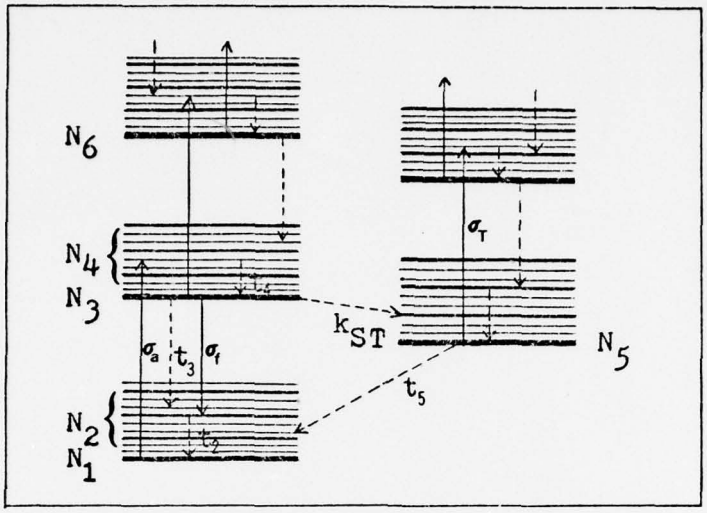

Figure II-1: Energy level diagram for a laser dye. Solid lines indicate radiative transitions, dashed lines indicate nonradiative transitions.

labeled N_2. The heavy lines in N_2 represent vibrational levels. N_2 typically has an energy range of 1400 to 1700 cm^{-1}. The energy spacing between rotational levels is smaller than the spacing between vibrational levels by a factor of approximately 100. The rotational levels provide a near continium of levels.

All other singlet and triplet states have similar associated manifolds. Because of these manifolds, the electronic levels are not sharply defined and absorb a broad range of wavelengths.

The first step of the laser process is the excitation of molecules from the ground state to N_4, the manifold of the first excited singlet state N_3. Transitions between singlet states are spin-allowed, giving rise to strong absorption bands. The molecule then decays nonradiatively to N_3. This nonradiative decay, also known as thermalization, occurs within picoseconds. The laser emission results from the

stimulated emission between levels N_3 and N_2. The laser process is completed by the nonradiative decay from N_2 to N_1.

The spontaneous decay from N_3 to N_2, known as fluorescence, occurs in nanoseconds for dye molecules. For solid-state and inorganic laser materials, the spontaneous decay time from the upper laser level is usually on the order of 10^{-3} seconds. This fast decay time essentially eliminates the possibility of Q-switching and requires very hard pumping to obtain lasing. Another characteristic of laser dyes is that although the emission and absorption bands are separate, there is usually still a region of overlap (see fig II-2). The dye is transparent to laser emission for much of the emission band but at the shorter wavelengths, reabsorption occurs. As will be shown later, reabsorption has important effects on injection locking.

Molecules in the excited singlet N_3 state may relax by a nonradiative process to a lower lying triplet state instead of decaying to the ground state. The triplet state is shown as N_5 in figure II-1. This process, known as intersystem crossing, proceeds at a rate called the intersystem crossing rate, k_{ST}. Intersystem crossing is indicated by a dashed line in figure II-1. It competes with fluorescence in the deactivation of N_3 and may have serious effects on the laser.

The lifetime for decay of the triplet state, N_5 to the ground state, denoted by t_5, is generally much longer than t_3 since the triplet-singlet transition is spin forbidden. This

means that molecules tend to hang up in the triplet states and lower the efficiency of the laser as will be discussed later. The actual value of t_5 depends upon the experimental conditions, particularly upon the amount of oxygen present in the dye solution, and may vary from 10^{-7} seconds in an oxygen saturated alcohol solution to 10^{-3} seconds in a degassed solution. The decay process N_5 to N_2 may be radiative or nonradiative. The radiation accompanying the process is termed phosphorescence. The triplet state acts as a trap for the excited molecules and depletes the supply of molecules available for the laser process because of its long lifetime.

Triplet-triplet transitions are spin-allowed and the optical absorption associated with these transitions is strong. Unfortunately, the corresponding absorption band generally overlaps the singlet state fluorescence spectrum. As a consequence, the accumulation of molecules in the triplet state produces a large optical loss at the wavelengths for which laser emission is most probable. Lasing has been attempted for the N_5 to N_2 transition but the triplet levels cannot be pumped efficiently enough to obtain lasing. The absorption associated with triplet process can be strong enough to quench or even prevent laser emission. In order to minimize the detrimental effects of the molecular triplet state it is necessary to reach laser threshold before a significant number of molecules have accumulated in the triplet state. Even though quenching techniques are used to keep the popula-

tion of the triplet states small an excitation source with an intensity that increases rapidly with time is often required. For that reason, there is a great advantage in using a giant pulse laser for excitation.

Optical absorption between excited singlet states, such as the process connecting N_3 and N_6 in figure II-1, is also a source of optical loss in the dye laser. The importance of this loss is seen only at high cavity fluxes where excitation can compete with the fast nonradiative decay times from N_6, which are on the order of 10^{-11} to 10^{-12} seconds. Low mirror reflectivities cause the necessary inversion to be larger and thus more molecules are available in N_3 for absorption (Ref 12:964).

Competition between fluorescence and other decay processes for the excited singlet state leads to a quantum yield for fluorescence, ϕ, defined as the ratio of the number of fluorescent photons emitted to the number of excitation photons absorbed. For most laser dyes, ϕ lies between 0.5 and 1.0. The actual value for a given dye depends upon the solvent, the temperature, and the other experimental conditions.

Rhodamine 6G

Figure II-2 shows absorption and emission curves for R6G in water and Ammonyx LO. Ammonyx LO is a detergent and is used to keep R6G and some other dyes from clumping in water. These curves are used to obtain the cross sections used later in this paper. The emission curve is assumed to be corrected for absorption and the absorption curve for emission since the paper they were taken from used them as such.

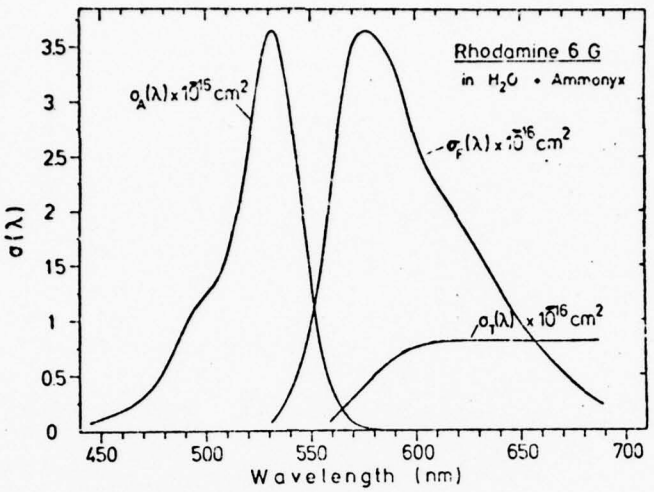

Figure II-2: Cross sections for absorption (σ_A), for fluorescence (σ_F) and for triplet absorption (σ_T) for rhodamine 6 G, dissolved in water with Ammonyx, a commercial surfactant, added.

The decay time for N_3 is 5.5×10^{-9} seconds, k_{ST} is 1.6×10^{7} sec^{-1}, and t_5 is 5.6×10^{-7} seconds (Ref 10:861). These are consistent with values found for Rhodamine 6G.

Injection Locking

Injection locking is an efficient technique for tuning a laser. Prisms, gratings, filters, and other tuning devices produce heavy losses within the cavity and greatly reduce the output power of the laser. In injection locking, tuning is accomplished by directing the output of a narrow band laser along the optical path of the laser to be tuned, not by introducing the loss mechanisms previously mentioned. The injection, which begins before the tuned laser is pumped, generates a strong preference for modes operating at the injected wavelength. The prefered modes contain most of the output energy of the laser. An untuned, pulsed dye laser normally has an output 40Å wide. In an experiment by Erickson and Szabo (Ref 4), 80% of the laser output was in a bandwidth of about

7 Å. The other 20% was spread out over other wavelengths with intensities 10^4 less than that of the desired output. Erickson and Szabo have achieved an output bandwidth .00016Å wide with the same output power as when the cavity is untuned.

Injection locking occurs when one mode is given an initial photon density greater than the spontaneous emission photon density in adjacent modes. This mode will then reach a larger photon density than the adjacent modes when the laser gain saturates. This is a consequence of the modes having the same gain during the oscillation growth period. If the injected photon density is much larger than the sum of the spontaneous emission densities in the oscillation modes, the output is controlled completely by the injected mode (Ref 4:434).

The injected signal depends on various operating parameters and conditions. The difference between the injected wavelength and the peak cavity wavelength, the pumping level used, the degree of coupling between the two cavities, and the cavity Q (Ref 17:443; 16:324). If pumping is at or just above threshold, spontaneous modes will require more buildup time and thus, locking is maintained for longer periods of time. The dependance on cavity Q and the wavelength difference can be seen in the following expression (Ref 16:324) for the locking range of an injection locked laser:

$$\delta\omega = \frac{\omega_o}{Q}\left[W(\text{injection})/W(\text{amplifier})\right] \qquad \text{II-2}$$

where ω_o is the cavity resonance frequency
Q is the cavity Q
W is the total laser power
$\delta\omega$ is the difference in the cavity and injection frequencies

If the gain of the laser amplifier is high enough and the injection is strong enough, then amplification can still occur for wavelengths which do not correspond to the axial modes of the amplifier and locking will occur for short times. As the coupling between the injection and amplifier cavities increases, then locking occurs for longer times.

The Amplifier

The amplifier used by A. A. Pease, O. G. Peterson, M. L. Spaeth, and W. M. Pearson has an optical path length of approximately 6cm, a dye gap of 1mm, and a dye flow rate of 1gal/min. A discharge heated copper vapor laser is used for pumping the amplifier and a narrow band dye laser is used for injection locking. Mode width of the amplifier output varied from 200-400 MHz (Ref 11:28-29).

The output amplitude from the ring varied in a random manner by a factor of ~3. The amplitude fluctuations were found to be strongly correlated with an accoustic vibration which existed in the mechanical structure of the device. The observed average conversion efficiency with the amplitude fluctuations present, was in excess of 40%. Peak energy conversion efficiency on a per pulse basis was ~60% (Ref 11:29).

The cube considered here is a design by Pease *et al* to suppress the accoustic vibration. The cube is 7.1x7.1x7.5mm and the slit is .45x7.4x3.72mm (fig II-3a). The surfaces of the cube are flat to within $\lambda/10$ at 630nm and the corners are square to within 2 sec of arc. The sides of the slit are flat to within $\lambda/4$ at 630nm, parallel to each other to within 20

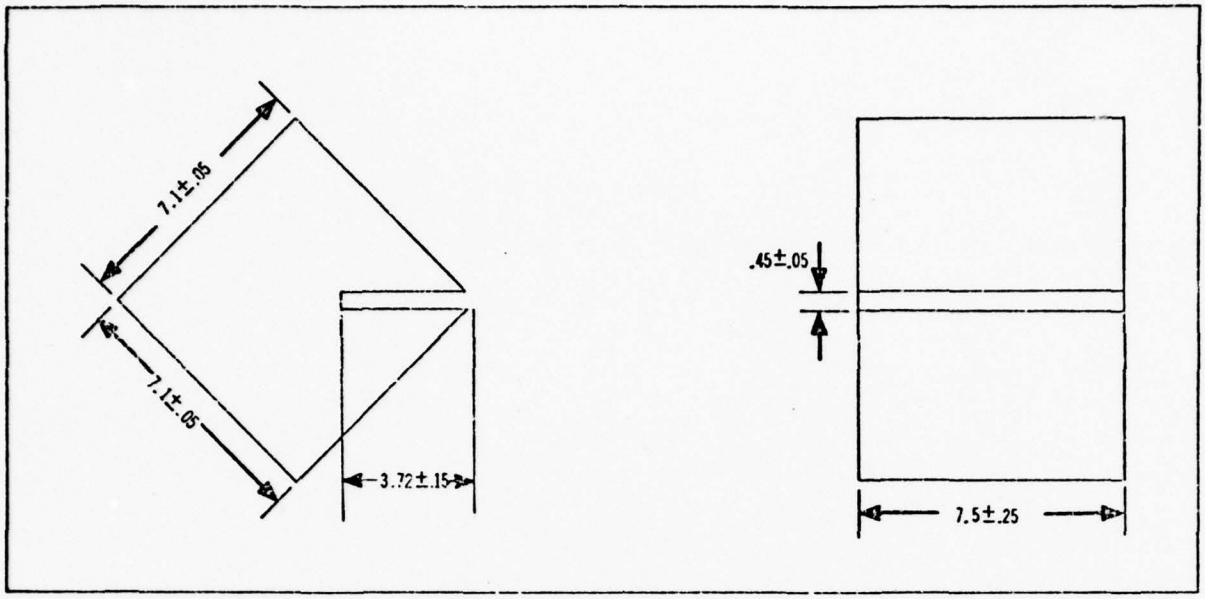

Figure II-3a: Laser Amplifier Cavity. All distances are in millimeters.

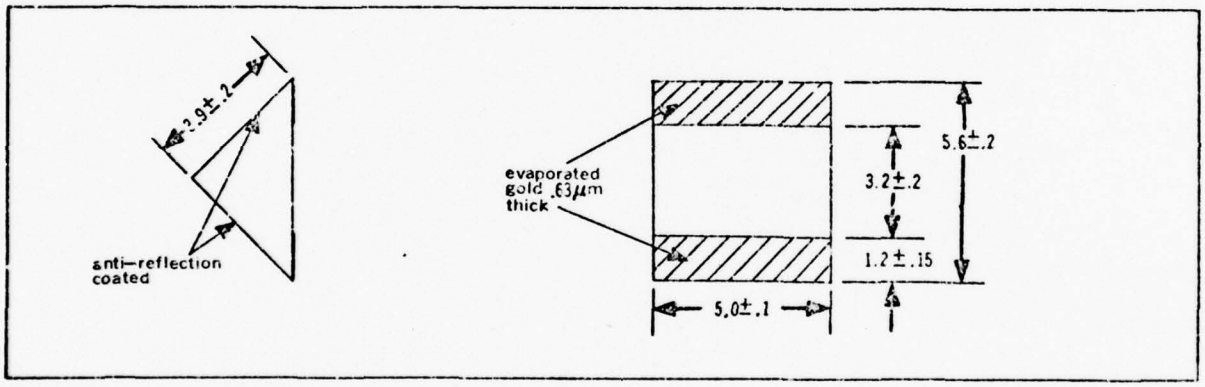

Figure II-3b: Ftir Prism. All distances are in millimeters

sec of arc, and at an angle of 45° to the sides of the cube to within 20 sec of arc.

The prism has sides of 4.2mm, a length of 5mm and a hypotenuse of 3.2mm. Two strips of gold evaporated on the prism provide spacing between the prism and the cube. The gold strips are 1.2mmx5mmx.62μm. Piezo-electric crystals press on the apex of the cube to vary the spacing between the cube and the prism. The sides of the prism are anti-reflection coated to less than .25% reflectivity for wavelengths between

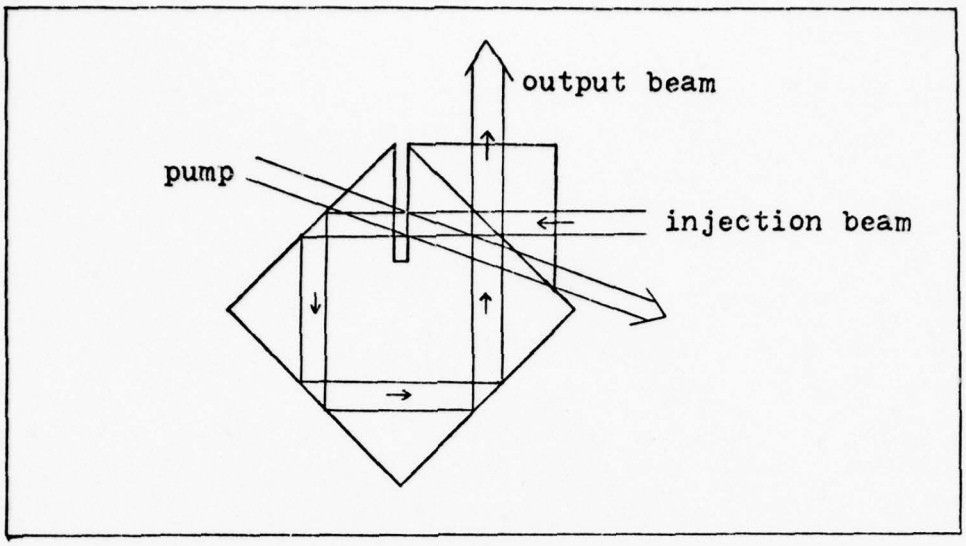

Figure II-4: Configuration for injection locking.

580 and 650nm. All angles are accurate to within 5min of arc.

The amplifier works on the principle of total internal reflection. The prism is used to frustrate the internal reflection and variable output coupling is obtained by changing the spacing between the prism and the cube. Figure II-4 is one possible configuration for the cavity. Variations can be made by changing where the pump beam enters and the placement of the prism.

The ratio of reflected to transmitted light for a polarization parallel to the plane of incidence and with an angle of incidence of 45° is (Ref 9:536):

$$\frac{R_p}{T_p} = \frac{(n^2-1)^4}{4n^2(n^2-2)} \cdot \sinh^2 \left[\frac{2\pi \cdot \delta x}{\lambda} \left[\frac{n^2-2}{2} \right]^{\frac{1}{2}} \right]$$

where δx is the spacing between the cube and prism
n is the index of refraction
R_p is the reflected radiation
T_p is the transmitted radiation

For n=1.474 and δx varying between 0 and 0.63μm, the reflectivity can be varied between 0 and 94%.

Relevant Material

Gerd Marowsky has discussed and analyzed the basic principles of dye laser operation using a modified, four-level rate equation approach (Ref 10). Using this approach, he has derived equations for the steady state laser efficiency and threshold pumping rates. Calculations have proved consistent with experimental results.

Chinlon Lin studied relaxation oscillations in dye lasers. He used linearized rate equations and small-signal approximation to describe the initial-spiking phenomenon present at the iniation of lasing. When compared against experimental results, his results show good qualitative agreement (Ref 7).

In an article written by U. Ganiel, A. Hardy, and D. Treves (Ref 5), injection locking in pulsed dye laser systems was discussed. They show that under pulsed conditions, injection locking can be accomplished over a wider range of parameters than under cw conditions. Their analysis is based on the solution of coupled rate equations for population densities and photon fluxes at all wavelengths. Their analysis is for both two-mirror and ring laser cavities.

The articles by Marowsky, Lin, and Ganiel *et al* provide the basis for the model developed in this paper and for supporting its validity. It is desirable to support a model by qualitative comparisons. This is not always possible and qualitative results must be relied upon. Marowsky provides qualitative

results for comparison. The articles by Lin and Ganiel do not provide the purely qualitative results that Marowsky does. Lin's results are still very useful because they predict characteristics of laser output for varying pump powers above threshold. The results by Ganiel *et al* are useful only in that they show characteristics of laser output as injection locking is broken.

III Theory

In this chapter, the rate equations to model the amplifier are derived. Certain transitions can be neglected in deriving the rate equations. These transitions and other assumptions are discussed and the rate equations are presented. The necessary additions to the rate equations are explained and then presented.

The Rate Equations

When analyzing dye lasers, it is generally not necessary to work with a set of rate equations in which every level appears explicitly. In most cases, appropriate simplifying assumptions greatly reduce the number of equations required for accurate calculations. Electronic levels higher than the first excited singlet and triplet levels are neglected. Intraband transitions can also be neglected along with spatial variations in the active medium. These assumptions are discussed in this section and lead to a general set of rate equations for dye lasers.

For this analysis, no singlet state higher than the first excited state need be considered. Excited singlet absorption is important only at high intensities (2×10^9 w/cm^2) (Ref 12:964) where the rate of absorption from the first excited singlet state, N_3, becomes comparable with the very fast nonradiative decay times from higher levels which are on the order of 10^{-11} to 10^{-12} seconds. Excited singlet absorption will decrease the output of the laser by 5% or less for mirror reflectivities of 70% or higher. This is due to the lowering of the laser

threshold and thus fewer molecules are in the upper laser level. For the purposes of this paper mirror reflectivities will be 95%.

The first triplet state is the only one considered in this paper. The higher triplet states are neglected because the decay times from those levels are on the order of 10^{-11} to 10^{-12} seconds; thus, except under very high flux conditions those levels remain empty (Ref 12:964).

The nonradiative transitions, N_4 to N_3 and N_2 to N_1, occur in picoseconds. Vibronic intra-band transitions are much faster than the combined spontaneous and stimulated rates from one electronic band to another, thus excluding hole burning effects in the vibrational-rotational manifold (Ref 10:858). These nonradiative transitions can be neglected. N_3 can be assumed to be pumped directly and N_2 remains empty.

Two additional assumptions are that there are no spatial variations in the active medium and that ϕ is 100%. The medium considered here is .45mm thick; even under conditions of high gain, the variations will be small (Ref 10:861). For R6G in water, ϕ is 95% and allowing ϕ to be 100% makes little difference in the results obtained (Ref 10:858).

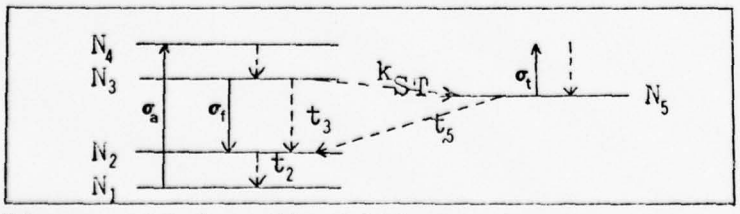

Figure III-1: Simplified energy level diagram

Since N_3 is assumed to be pumped directly from the ground state, no rate equation for N_4 need be written. The equation for N_3, the upper laser level, must include terms for pumping, reabsorption, stimulated and spontaneous emission, and intersystem crossing. Equation III-1 is for dN_3/dt. The first term in III-1 is the pump term, W. The second term is for stimulated emission. The number of photons within the cavity is q, σ_f is the cross section for stimulated emission, N_3 is the density of molecules in the upper laser level, c is the speed of light in a vacuum, and v is the volume of the pumped dye. The third term accounts for reabsorption and σ_a is the cross section for absorption. The fourth term is for spontaneous decay. The last term accounts for intersystem crossing,

The equation for the triplet level, N_5, contains two terms, accounting for intersystem crossing and decay to N_2. The first term in eq III-2 is for intersystem crossing and the last term is for decay.

Equation III-3 is for the change in the number of photons within the cavity with time. Eq III-3 accounts for stimulated emission, photons lost due to output coupling, and singlet and triplet absorption. The first term on the right is for stimulated emission. The second term is for the cavity losses. T_i is a dimensionless term which accounts for scattering, diffraction, absorption and other losses (Ref 10:860). The rest of the second term accounts for output coupling losses where L is the optical path length of the cavity. The third and fourth terms are for singlet and triplet absorption respectively.

The last equation, III-4, is for conservation of molecules. N is the density of molecules in the active medium. N_1, N_3, and N_5 are the density of molecules in the ground state, upper laser level, and the triplet state respectively.

$$dN_3/dt = W - q\cdot\sigma_f\cdot N_3\cdot c/v + q\cdot\sigma_a\cdot N_1\cdot c/v - N_3/t_3 - k_{ST}\cdot N_3 \qquad \text{III-1}$$

$$dN_5/dt = k_{ST}\cdot N_3 - N_5/t_5 \qquad \text{III-2}$$

$$dq/dt = q\cdot(\sigma_f\cdot c\cdot N_3 - (T_i+\ln 1/R)\cdot c/L - \sigma_a\cdot c\cdot N_1 - \sigma_T\cdot c\cdot N_5) \qquad \text{III-3}$$

$$N = N_1 + N_3 + N_5 \qquad \text{III-4}$$

Equations for Injection Locking

For the analysis of injection locking and to allow for delocking to occur, additions are made to the rate equations to allow for the cavity to oscillate at two wavelengths and to include the injected photons. The equations which result are similar to those used by Maeda *et al* except that triplet reabsorption is accounted for (Ref 8:1732).

The first change is to equation III-1. Two terms are added which allow for the stimulated emission and reabsorption of the injected photons, p. In the new equation for dN_3/dt, σ_{aq} and σ_{ap} are the cross sections for singlet reabsorption for the spontaneous cavity mode and the injected mode respectively. σ_{fq} and σ_{fp} are the cross sections for stimulated emission for the spontaneous and injected modes.

The second change is to add a photon rate equation for p, the injected wavelength. The cross section for triplet absorption is σ_{Tp}. The new equations are as follows:

$$dN_3/dt = W + q \cdot \sigma_{aq} \cdot N_1 \cdot c/v + p \cdot \sigma_{ap} \cdot N_1 \cdot c/v - N_3/t_3 - q \cdot \sigma_{fq} \cdot N_3 \cdot c/v - p \cdot \sigma_{fp} \cdot N_3 \cdot /v \quad \text{III-5}$$

$$dN_5/dt = k_{ST} \cdot N_3 - N_5/t_5 \quad \text{III-6}$$

$$dp/dt = p \cdot (\sigma_{fp} \cdot c \cdot N_3 - (T_i + \ln(1/R)) \cdot c/L - \sigma_{ap} \cdot c \cdot N_1 - \sigma_{Tp} \cdot c \cdot N_5) \quad \text{III-7}$$

$$dq/dt = q \cdot (\sigma_{fq} \cdot c \cdot N_3 - (T_i + \ln(1/R)) \cdot c/L - \sigma_{aq} \cdot c \cdot N_1 - \sigma_{Tq} \cdot c \cdot N_5) \quad \text{III-8}$$

$$N = N_1 + N_3 + N_5 \quad \text{III-9}$$

A constant value of 10^{-6} of the spontaneous decays from the upper laser level are assumed to go into the spontaneous cavity mode. Juramy, Piere, and Meyer found that the constant used is unimportant (Ref 6: 858).

For the purposes of this paper, one mode is assumed to start spontaneously. Maeda *et al* used the same approach by assuming that the gain and cavity lifetime are the same for all of the cavity modes (Ref 8:1731). The same assumption is used here for solving the rate equations. The cross sections for emission and absorption are averaged for a 40 Å band centered at 590nm. This band encompasses the peak of the emission band and is where spontaneous emission is most likely to occur. The result is that the output at that wavelength becomes the sum of the wavelengths in that 40 Å band.

IV Results and Discussion

This chapter has two purposes. The first is to obtain support for the model developed in this paper. This is done by comparing calculations using the rate equation model to the work of Marowsky, Lin, and Ganiel *et al*. The second is to present and discuss the results obtained for calculations of injection locking using the rate equation model for varying conditions. The rate equations are solved using the integrator discussed in Appendix A.

Results for Comparison

The model is compared to work by three authors for conditions of steady state, pulsed, and injection locked operation. Comparison is done with Marowsky for steady state operation. Calculations are made for six conditions using his equation for laser efficiency and using the model developed here. The operating parameters are the same as those used by Marowsky except that a different pump rate is used which has no effect on the laser efficiency. The efficiencies obtained from the two sets of calculations are then compared to find any significant differences. For pulsed conditions, the work by Lin is used for comparison. The parameters used by Lin are used here and the results are compared. Quanitative analysis is not possible, but times at which spiking occurs after the pumping starts, the characteristics of the spikes which occur, and the shape of the output pulse for varying pump rates can be compared. For conditions of injection locking, the work by

Ganiel *et al* is used. The exact parameters they used cannot be used here because not all of the parameters could be obtained. What is done then, is to reproduce the conditions they used as closely as possible and then compare the results. The only area which can be compared are the characteristics of the output as injection locking is broken with and without triplet absorption.

Marowsky obtained an equation for the efficiency of a dye laser (Ref 10:861) which is given in equation IV-1. He obtained solutions for the efficiency of the laser at wavelengths of 560, 590, and 620nm for conditions with and without reabsorption. The cross sections for stimulated emission, singlet absorption, and triplet absorption are shown in Table IV-1. These cross sections are obtained from Fig II-2.

$$\eta = \lambda_{pump}/\lambda_{laser} \cdot T \cdot f \cdot \frac{1 - k_{ST} \cdot t_5 \cdot \sigma_T/\sigma_f}{T_u + D \cdot N \cdot \sigma_T \cdot k_{ST} \cdot t_5 \cdot \sigma_a/\sigma_f} \qquad \text{IV-1}$$

where $T = \ln(1/R)$

$T_u = T_i + \ln(1/R)$

D = the optical length of the cavity

$f = 1 - \exp(-N \cdot D \cdot \sigma_A(\lambda_p))$

λ_p = the pump wavelength

λ(nm)	σ_f($\times 10^{-16}$ cm^2)	σ_a($\times 10^{-16}$ cm^2)	σ_T($\times 10^{-16}$ cm^2)
560	2.25	.4	.1
590	3.3	0.	.6
620	2.0	0.	.8

Table IV-1: Wavelengths and cross sections used in computations for comparison with Marowsky.

other parameters for the system are as follows (Ref 10:861)

$k_{ST} = 1.7 \times 10^7$ sec^{-1}

$t_3 = 5 \times 10^{-9}$ sec

$D = .1cm$

$N = 1.4x10^{17} cm^{-3}$

$T_i = .05$

$R = .95$

$t_5 = 5.6x10^{-8} sec$

and $\lambda_p = 530nm$

The efficiencies obtained for calculations using Eq IV-1, the parameters given above, and the cross sections in Table IV-1 are shown in Table IV-2.

λ (nm)	$\sigma_a, \sigma_T=0$	$\sigma_a, \sigma_T\neq0$
560	.479	.377
590	.455	.38
620	.433	.277

Table IV-2: Efficiencies obtained using Marowsky's equation for laser efficiency.

The general set of rate equations (Eq III-1, 2, 3, and 4) are then integrated to a state as close to steady state operation as possible. The time required to go to steady state is excessively long for the cases where reabsorption occurs and so the equations are integrated until they come close to steady state. The plots for the computer runs are shown in Appendix B. The ratio of the number of photons out to those in times the quantum efficiency is taken to find the efficiency of each run. These efficiencies are shown in Table IV-3. A comparison between Table IV-2 and IV-3 show that variations are less than 2%. The differences are probably due to the type of integrator used but are small enough not to be significant. This close agreement lends support to the model for steady state conditions.

λ(nm)	$\sigma_a = \sigma_T = 0$	$\sigma_a, \sigma_T \neq 0$
560	.477	.374
590	.453	.38
620	.431	.281

Table IV-3: Efficiencies obtained using the model developed in this paper.

Chinlon Lin assumes constant cavity conditions and varies the pump rate between 10 and 750 times the threshold pump rate. The pump pulse Lin assumes is trapexoidal. Lin also assumes an ideal four level laser (Ref 7:603). By solving the rate equations for an ideal four level laser system, the threshold pump rate, W_t, can be obtained. W_t is given by:

$$W_t = \frac{N_o}{t_3} \qquad \text{IV-2}$$

where N_o is the threshold inversion above which $dq/dt > 0$ (Ref 7:603). The cavity conditions assumed by Lin are as follows (Ref 7:607):

$$t_c = 5 \times 10^{-11} \text{ sec}$$

$$t_3 = 2 \times 10^{-9} \text{ sec}$$

where t_c is the cavity decay time.

Lin's results are shown in figure IV-1 (Ref 7:607). The times at which the initial spikes occur and the time for sucessive major spikes is given in Table IV-4. As can be seen from Fig. IV-1, at very high pump rates, the output pulse begins to closely resemble the pump pulse used. The damping of the oscillations is roughly approximated by exponential decay (Ref 7:606).

Other than the conditions given above, Lin leaves many cavity conditions such as N, σ_f, and V undefined. The W_t

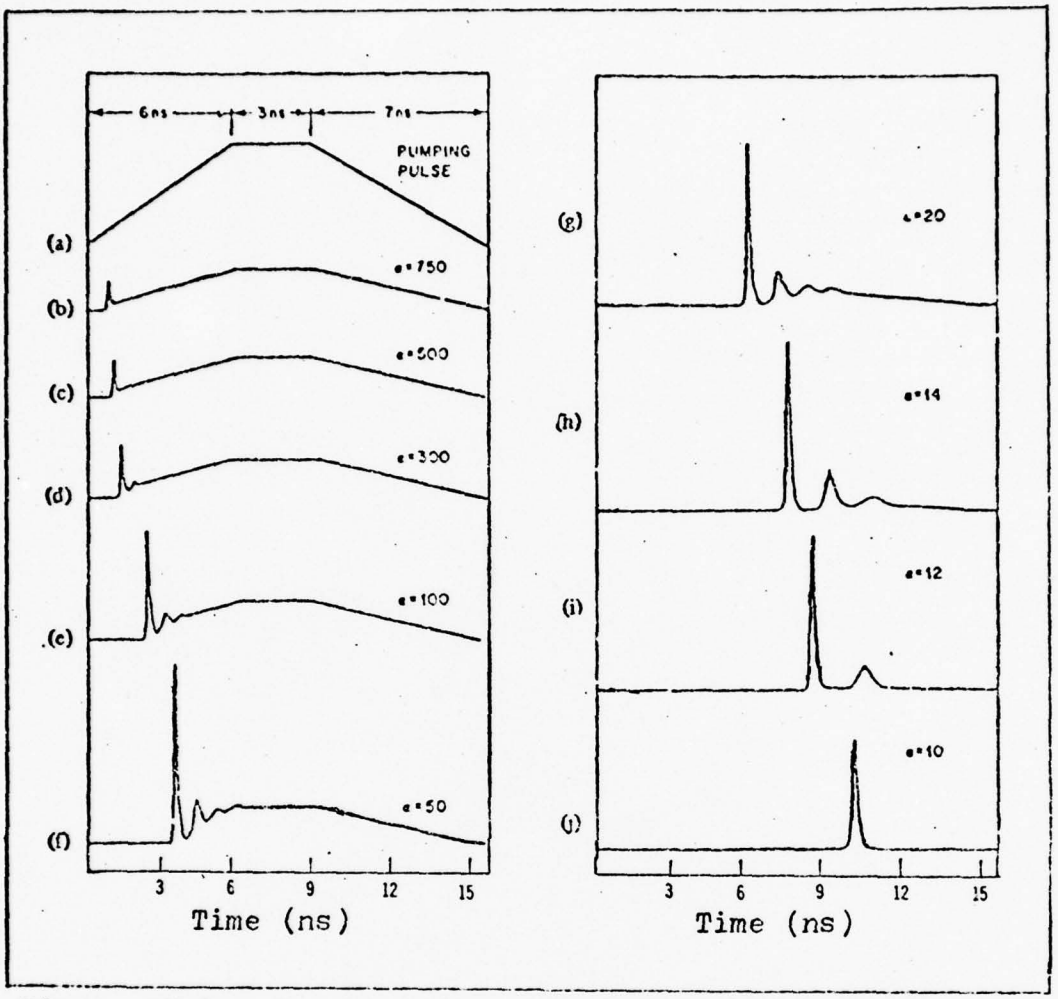

Figure IV-1: Results of C. Lin (Ref 7:607). t_c is 50ps, α is the sevel of pumping above threshold and is indicated for each plot. Figure (a) is the pump pulse used.

α	first spike	second spike	third spike
10	10 ns	-	-
12	8.5 ns	10.6 ns	-
14	7.6 ns	9.3 ns	10.8 ns
20	6.1 ns	6.7 ns	8.5 ns
50	3.5 ns	4.4 ns	5.0 ns
100	2.3 ns	3.2 ns	-
300	1.5 ns	1.8 ns	-
500	1.0 ns	-	-
750	.8	-	-

Table IV-4: Times at which spikes occur for varying pump rates above threshold (α).

calculated depends on N and σ_f, but the results are really only dependant upon the W_t calculated. For the calculations using the model developed here, a $3x10^{-4}$ molar solution is used and σ_f is chosen to be $3.3x10^{-16}cm^2$. Using Eq III-3 and neglecting reabsorption, the population density required for N_3 is:

$$N_3 = \frac{1}{\sigma_f \cdot c \cdot t_c} = 2.02x10^{15}cm^{-3}$$

N_3 times the volume of the active medium is the population inversion required. Using Eq IV-2, the critical pump rate is $V(1.01x10^{24}sec^{-1}cm^{-3})$. Lin does not specify a volume and here it is chosen to be $1cm^3$. This makes W_t equal to $1.01x10^{24}sec^{-1}$.

Using the conditions given above in the model and using pump rates 10, 12, 14, 20, 50, 100, 300, 500, and 750 times the threshold pump rate, the results in Fig IV-2 and Appendix C are obtained. The time at which the spikes occur are given in table IV-5.

α	first spike	second spike	third spike
10	-	-	-
12	11.1ns	-	-
14	9.1ns	-	-
20	6.9ns	9.0ns	11.2ns
50	4.2ns	5.4ns	6.5ns
100	3.0ns	4.0ns	4.8ns
300	1.9ns	2.6ns	3.2ns
500	1.6ns	2.1ns	-
750	1.3ns	1.9ns	-

Table IV-5: Times at which spikes occur for varying pump rates above threshold (α). For the model derived in this paper.

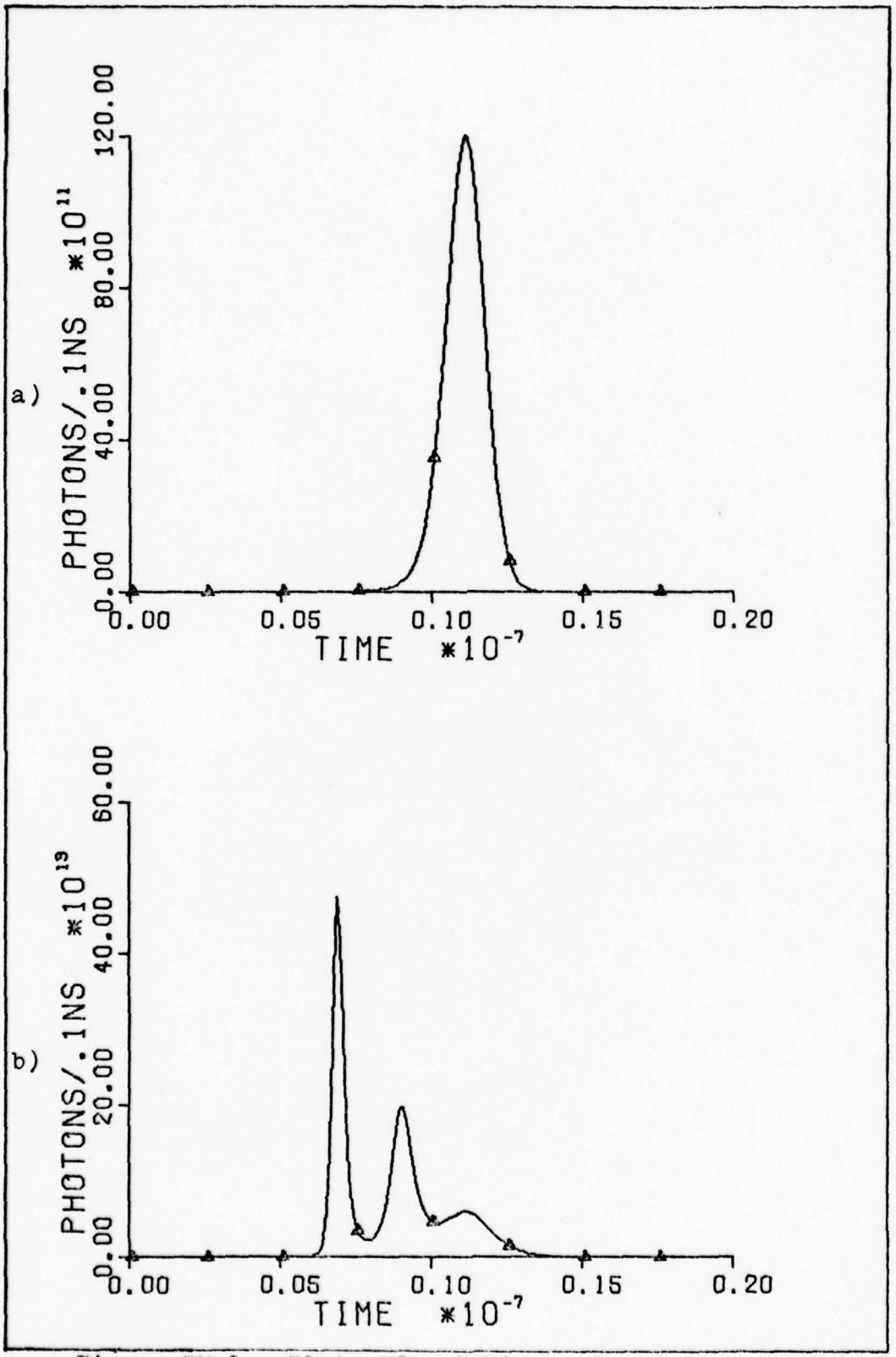

Figure IV-2: Plots of solutions of the rate equations. Fig (a) is for 12 times threshold and (b) is for 20 times threshold.

The first result is that lasing does not occur for ten times the threshold pump rate. This is because the inversion does not become large enough for lasing to occur. The inversion reaches 1.87×10^{15} which is 92% of the required inversion.

The second result is that the first spike in each calculation for the model occurs at a time later than the first spike in Lin's calculations by .5 to 1.01ns. In addition, calculations for 12 and 14 times the threshold pump rate do not have spikes occuring after the first spike, while those for Lin do. This is because the inversion does not build fast enough for spiking to occur before the pump pulse falls off. This is born out by the fact that the spacing between spikes from the calculations are much longer than the spacing between the spikes in Lin's calculations.

An additional result is obtained from semi-log plots of the results shown in figure IV-3 and Appendix C. The damping of the oscillations is exponential which is consistent with Lin and experimental results (Ref 7:606).

The most probable reason for the differences between Lin's work and the results here is the integrator used. The integrator is a first order Taylor expansion (see Appendix C) and error can be as large as 10% (Ref 19). The results for conditions near steady state are good, but the integrator apparently cannot handle the rapid changes of pulsed operation as easily. A more precise integrator may work better, but because of time constraints, this connot be verified.

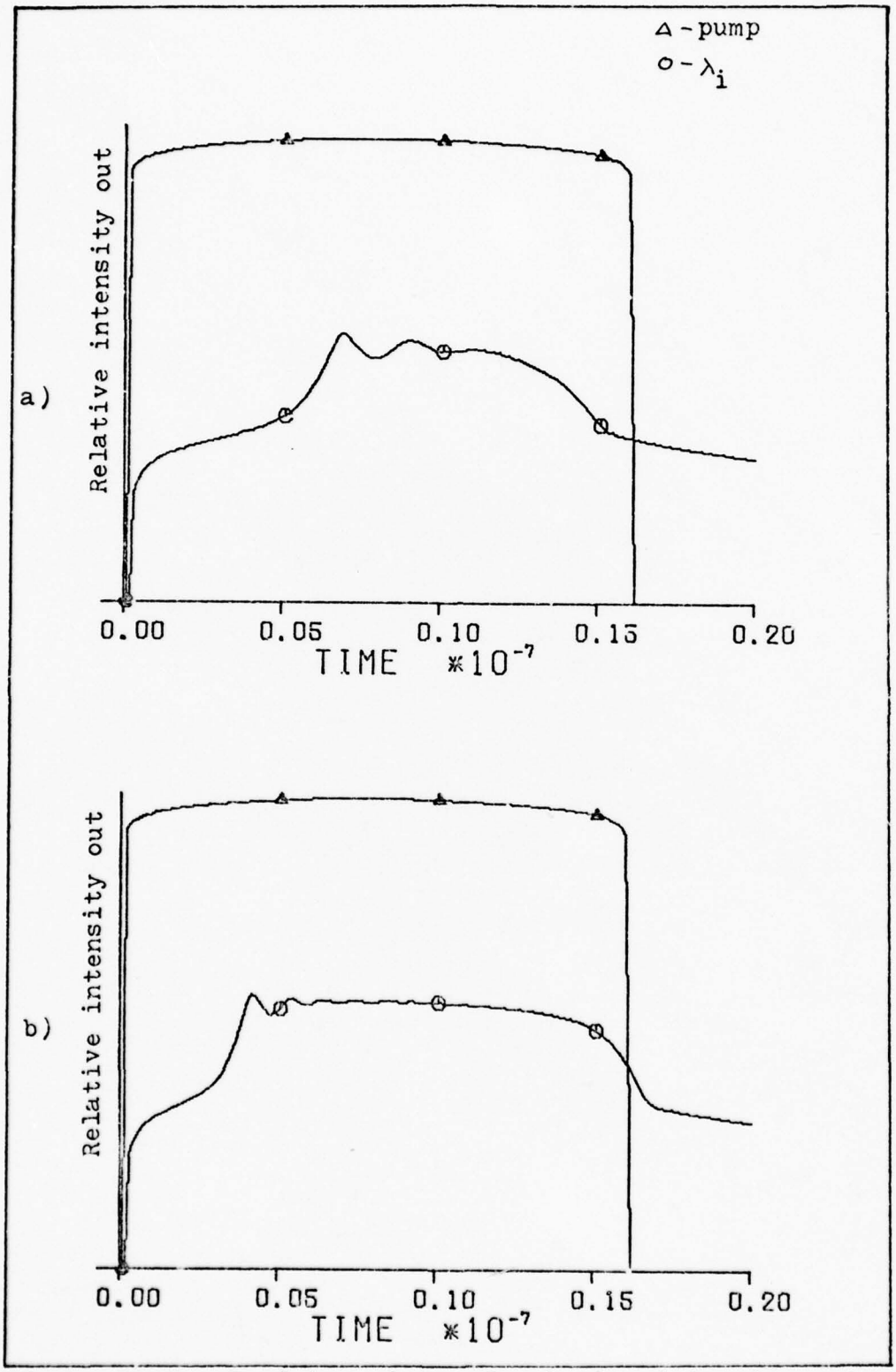

Figure IV-3: Semi-log plots of relative intensity out vs. time to show the exponential damping of the oscillations. Fig (a) is for 20 times the threshold pump rate and (b) is for 50 times the threshold pump rate.

As long as the pump rate is between 20 and 300 times the threshold pump rate, agreement between the results here and Lin's is within 80%. This is not as good as desired, but the model and the integrator are still useful as long as the pump rate remains within the bounds given above and for steady state.

The work of U. Ganiel *et al* is used for comparison for conditions of injection locking. The calculations are for Rhodamine 6G in ethanol at a 5×10^{-3} molar concentration. Injection is at 585nm and the spontaneous cavity mode is at 590nm. They use a delay time between the injection and pump pulses of 1ns. Additional parameters they use are as follows:

$t_3 = 5.5 \times 10^{-9}$ sec

$k_{ST} = 3.4 \times 10^{6}$ sec^{-1}

$t_5 = 2.5 \times 10^{-7}$ sec

$N = 3 \times 10^{18}$ cm^{-3}

$R = 20\%$

The cross sections for absorption and emission are not given in their paper and the reference given for where they are taken from is incorrect.

Their results are given in Figure IV-4 for a constant pump rate and injection pulse. In Figure IV-4a, triplet absorption is neglected. The buildup of the spontaneous cavity mode, λ_1, is exponential as is the decay of the injected mode, λ_i. Figure IV-4b shows the result for calcu-- lations where triplet absorption is accounted for. It can be seen that λ_1 builds but does not become more intense than

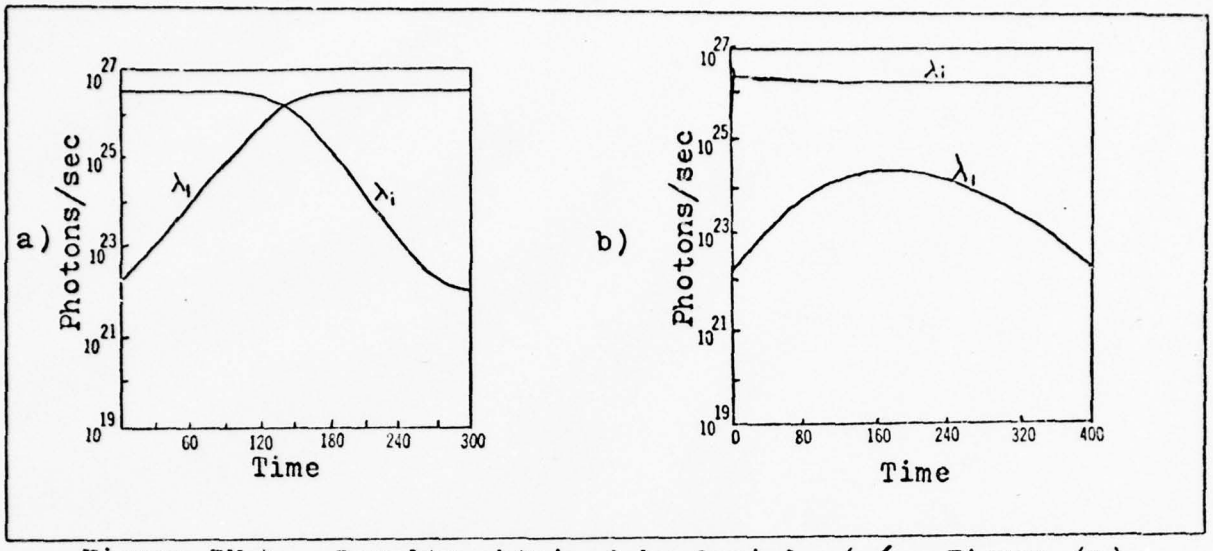

Figure IV-4: Results obtained by Ganiel *et al.* Figure (a) excludes triplet reabsorption and (b) includes it.

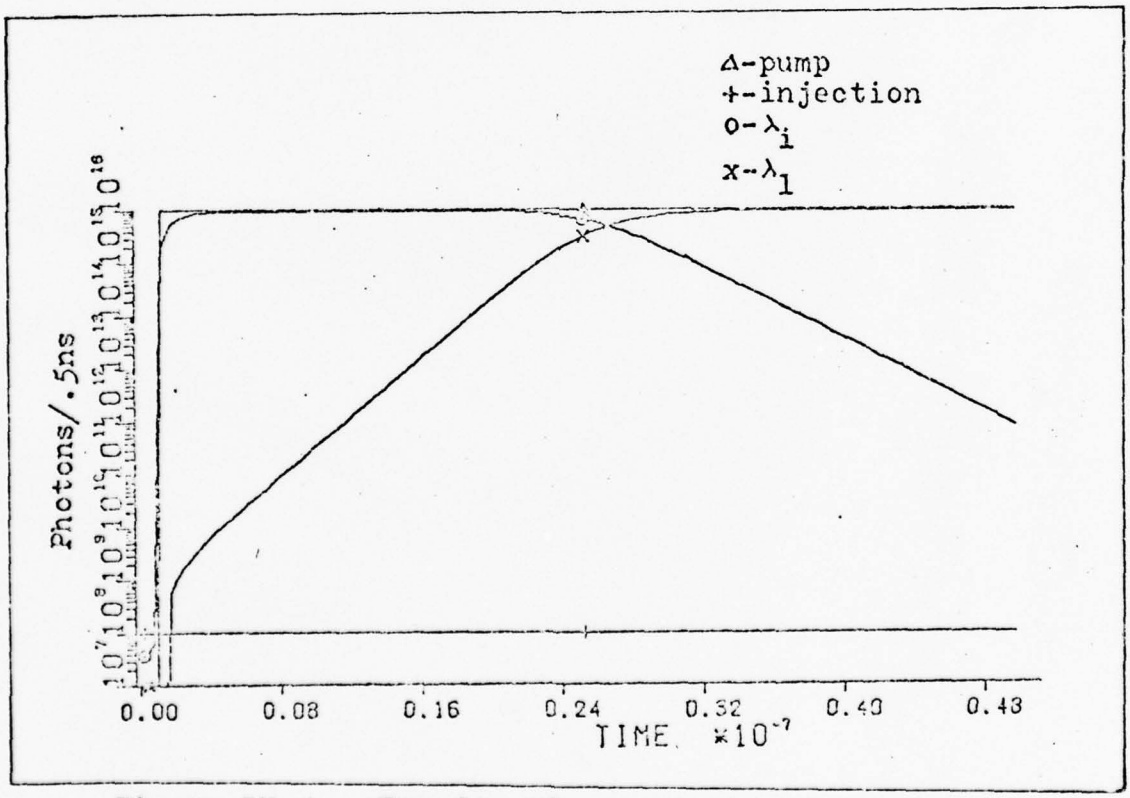

Figure IV-5 : Results of computation for injection locking obtained from the model developed in this paper.

λ_i and break the locking. This is the behavior desired in the solutions using the model for injection locking.

The cross sections they used cannot be obtained and the next best thing is done. The cross sections for absorption and emission are taken from Fig II-2. The cross sections are given in Table IV-6.

λ (nm)	$\sigma_f x10^{-16} cm^2$	σ_a	$\sigma_t x10^{-16} cm^2$
585	3.4	0	.55
590	3.3	0	.6

Table IV-6: Cross sections for Rhodamine 6G in water taken from Fig II-2.

The results of the calculations for the model are shown in Fig IV-5. It is shown that λ_1 builds exponentially and that λ_i decays exponentially after locking is broken. In figure IV-6, it can be seen that that as the injected pulse decays due to triplet absorption and the effects of the spontaneous mode, the spontaneous mode builds. After .9 sec, the triplet absorption is strong enough to quench lasing. There is no peak for the spontaneous mode and then the fall off as shown by the work of Ganiel *et al* before the triplet states quench lasing. This is due the the different cross sections used and the integrator. It can be seen however, that the buildup time required for the spontaneous mode is very long.

Comparison of the results here and the results of Ganiel *et al* shows only that the injected modes have similar characteristics when locking is broken and that the spontaneous modes also have similar characteristics. Also shown is that the time

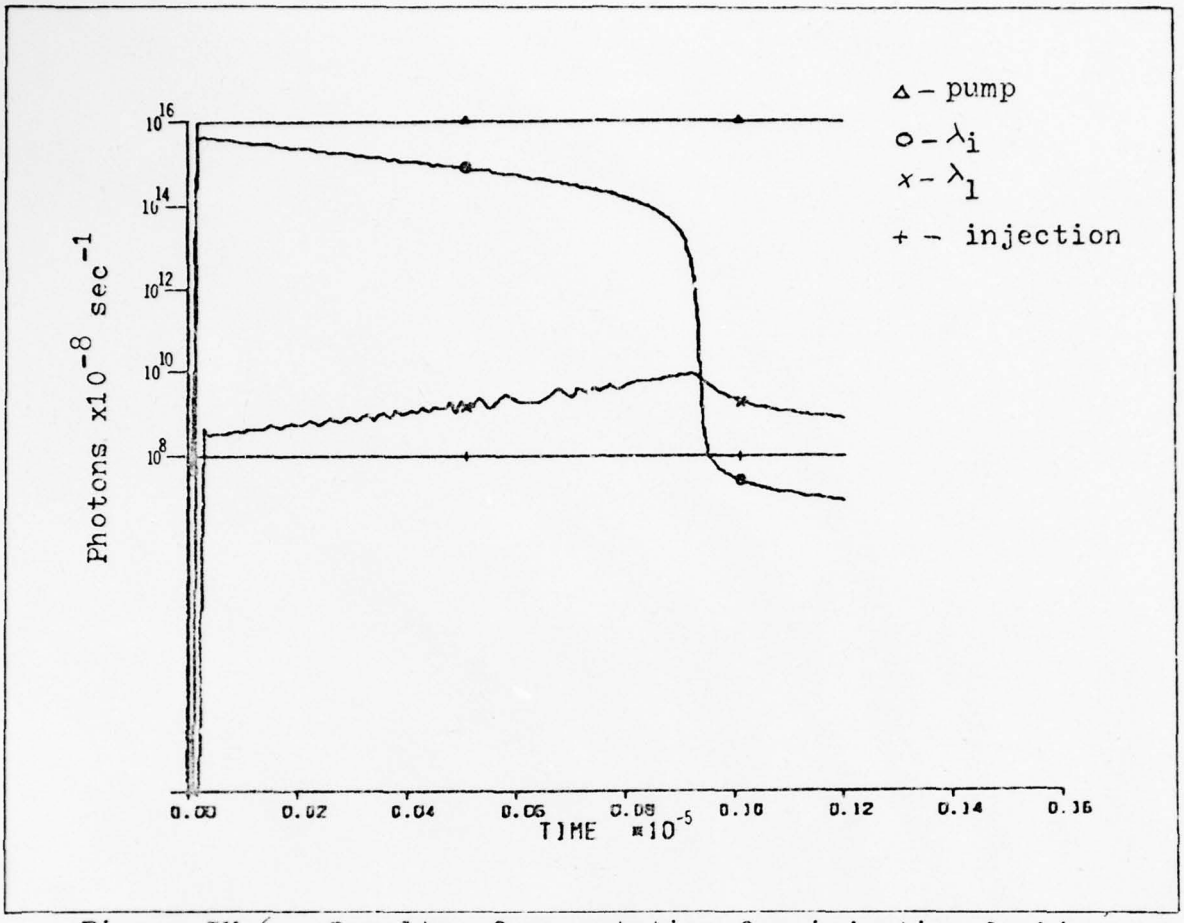

Figure IV-6: Results of computation for injection locking. Triplet absorption is included.

required for the spontaneous modes to break locking is very long when triplet absorption occurs. The result is that the two sets of results agree qualitatively.

Results for Injection Locking and Discussion

The model is now used for analysis of injection locking for varying wavelengths, delay times, and mirror reflectivities. The wavelengths used are shown in table IV-7 and 590 is the spontaneous cavity mode. Delay times between the injected and pump pulse are 1, 3, 5, 7, or 9ns. Table IV-7 also gives the cross sections used for the analysis. They are taken from Fig II-2.

λ(nm)	$\sigma_a x10^{-16} cm^2$	$\sigma_T x10^{-16} cm^2$	$\sigma_f x10^{-16} cm^2$
560	.4	.1	2.3
580	.05	.5	3.6
590	.01	.6	2.8
600	0.	.75	2.6
620	0.	.75	2.0

Table IV-7: Cross sections used for computer analysis.

The pump and injection beam areas are taken to be .04 cm^2. The pump energy density is 94 mj/cm^2 deposited over a time of 20 ns. The injection beam energy densities are given in Table IV-8.

λ(nm)	Energy (mj/cm^2)
560	.88
580	.867
600	.828
620	.802

Table IV-8: Injection beam energy densities.

The rate equations are solved over 35ns periods in .5nm time steps. Additional parameters are as follows:

$t_5 = .5625x10^{-7}$ sec

$k_{ST} = 1.6x10^{7}$ sec^{-1}

concentration = $2.4x10^{-4}$ mole/liter

$t_3 = 5.5x10^{-9}$ sec

R = 95%

Plots of the results of the calculations are given in Figures IV-7 through 11 and Appendix D. The plots in Figs IV-7 through 10 are for each wavelength considered at a delay time of 5ns.

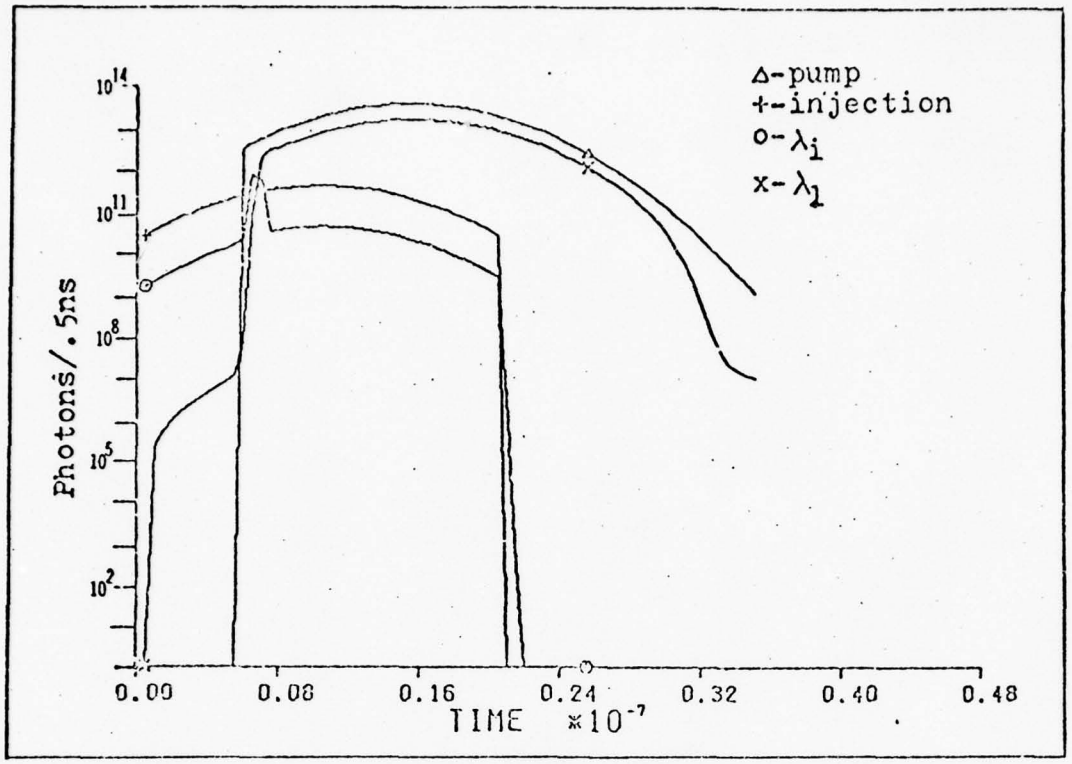

Figure IV-7: Computer solution for a delay time of 5 ns, λ_i is at 580 nm, and λ_l is at 590 nm.

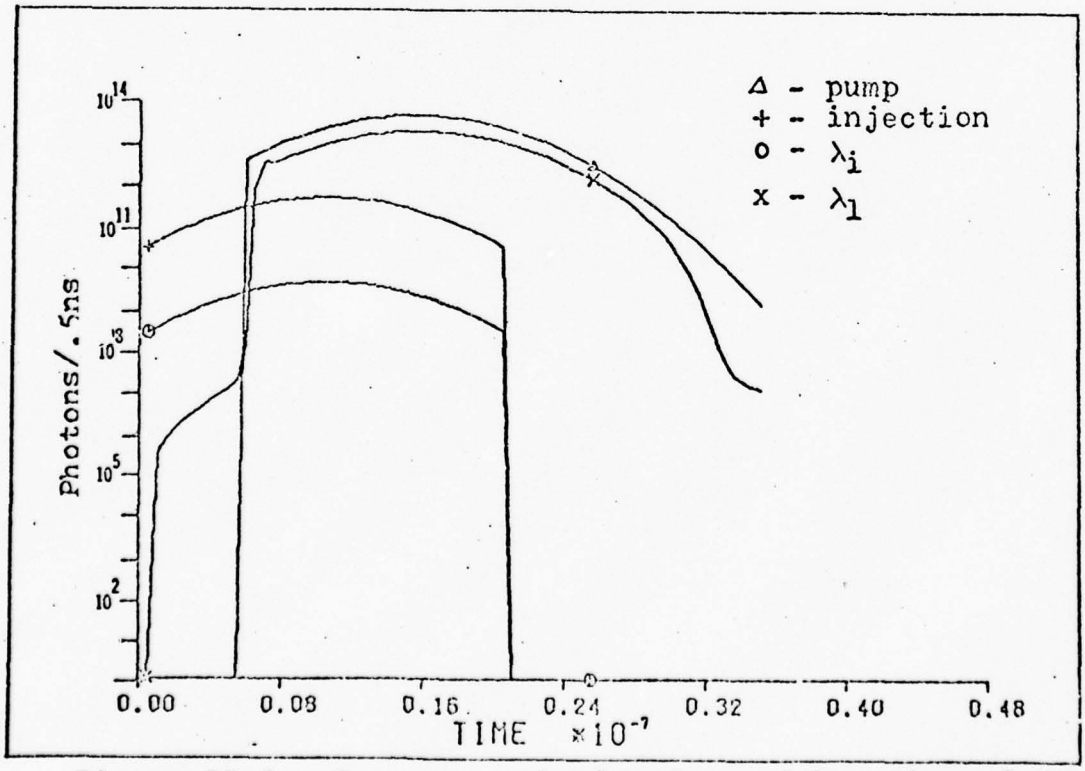

Figure IV-8: Computer solution for a delay time of 5 ns, λ_i is at 560 nm, and λ_l is at 590 nm.

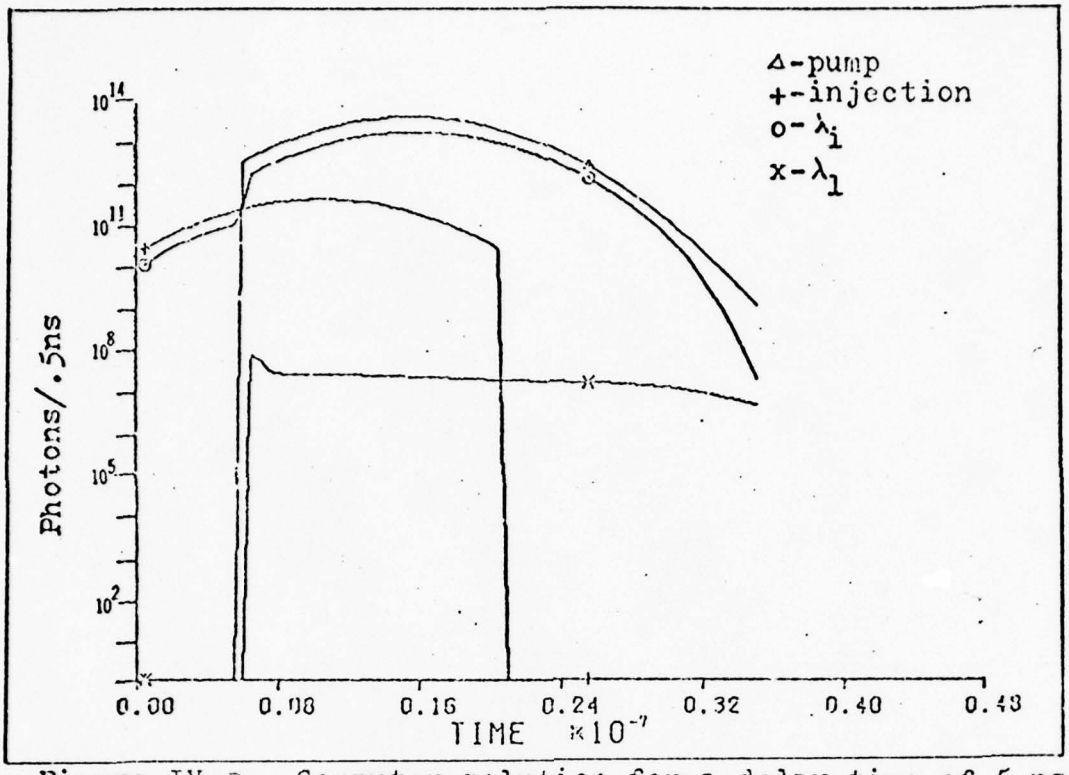

Figure IV-9: Computer solution for a delay time of 5 ns, λ_l is at 590 nm, and λ_i is at 620 nm.

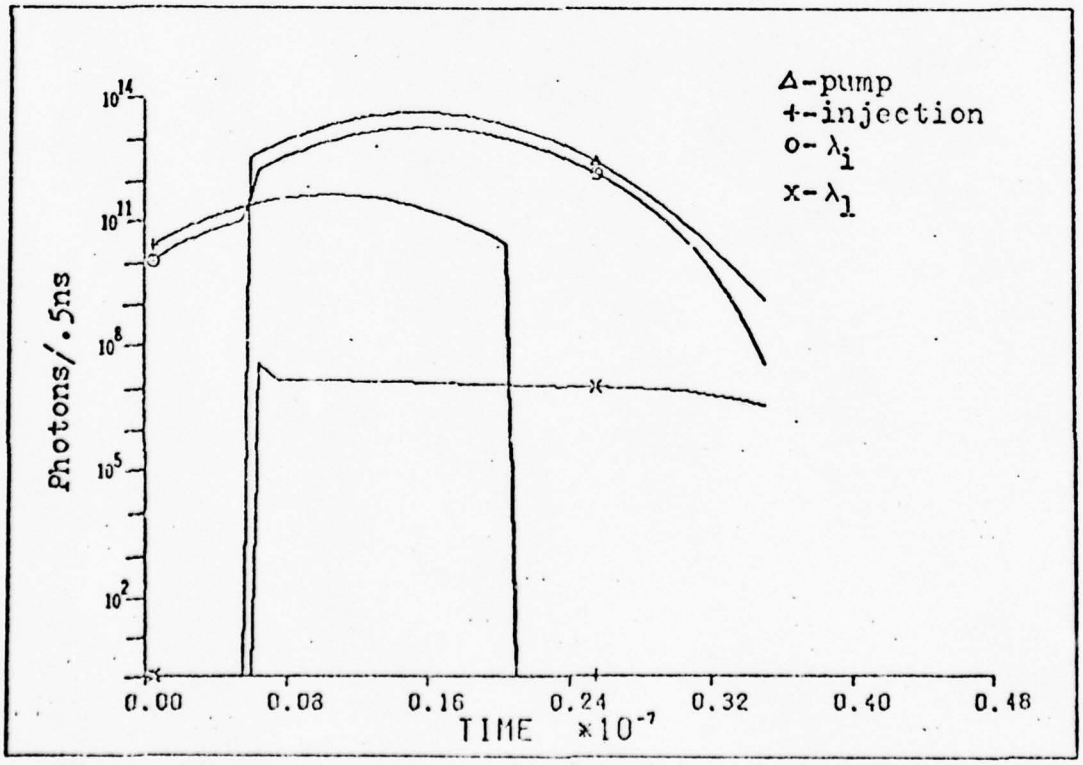

Figure IV-10: Computer solution for a delay time of 5 ns, λ_l is at 590 nm, and λ_i is at 600 nm.

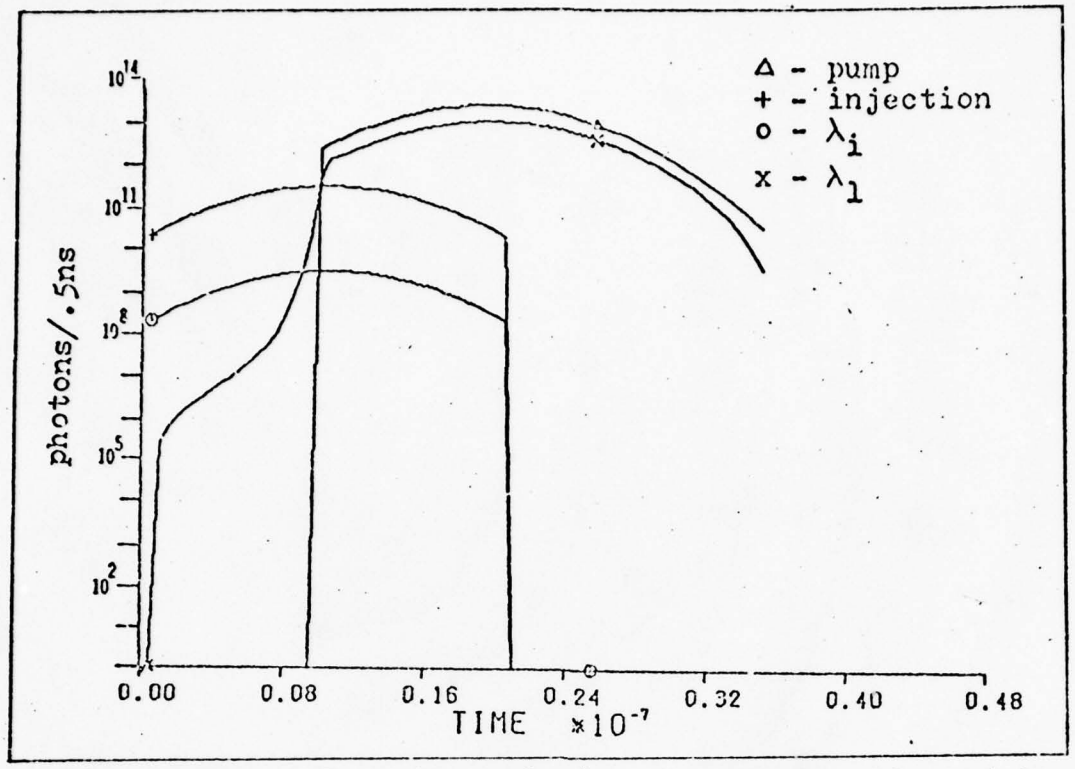

Figure IV-11: Computer solution for a delay time of 9 ns, λ_i is at 560 nm, and λ_l is at 590 nm. The injection causes the cavity to begin lasing at 590 nm due to the strong reabsorption and λ_i.

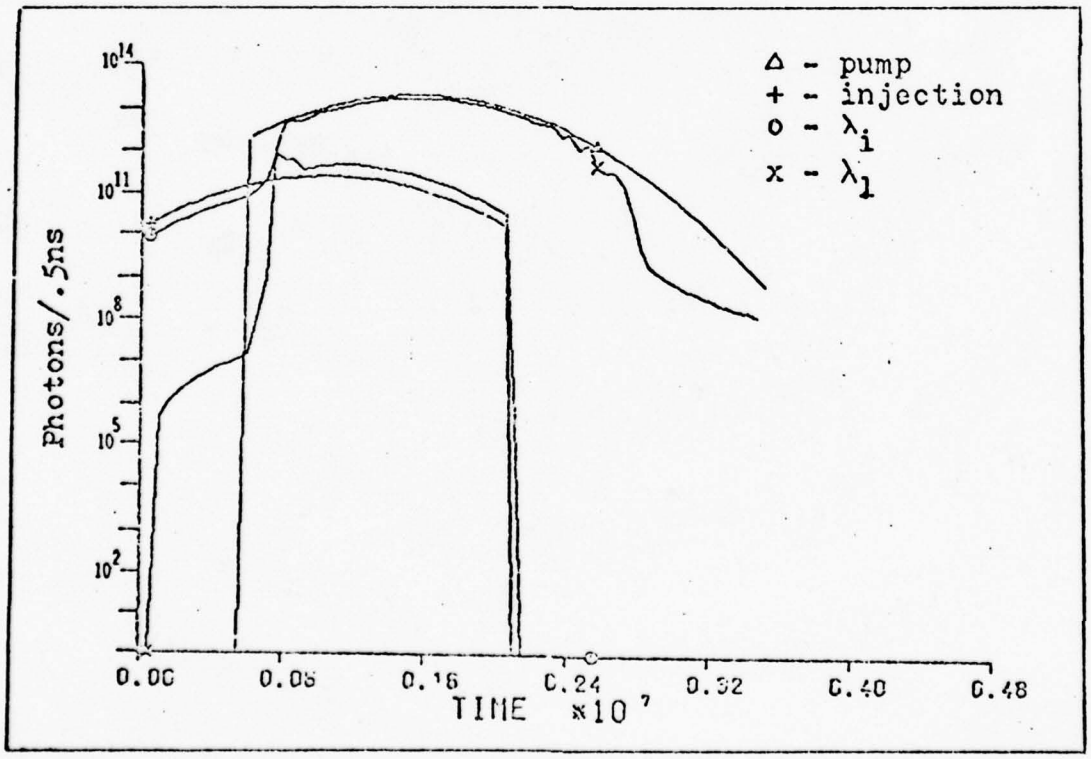

Figure IV-12: Computer solution for a delay time of 5 ns, λ_i is at 580 nm, λ_l is at 590 nm, and the mirror reflectivity is 20%. Injection locking is still not achieved, but the output at the desired wavelength is larger than that obtained for mirror reflectivities of 95%.

The first result is that where there is any singlet absorption at the injected wavelength, injection locking does not occur (Figs IV-7 and 8). An explanation for this is that for the small amplifier cavity considered here and under high mirror reflectivities, much of the energy in the injected wavelength is reabsorbed while the dye remains transparent to the spontaneous mode.

The active medium is .0648cm thick optically and the amplifier has an optical path length of 1.04cm. The decay time for the amplifier is 6.7×10^{-10} sec. In that time, light will travel 13.89cm and will therefore make 13 complete passes through the medium before the intensity falls off by one-half. This about the same as making one pass through a medium .84cm thick. The amount lost due to reabsorption becomes approximately:

$$1-\exp(-D \cdot \sigma_a \cdot N_1)$$

$$= .96.5\% \text{ at } 560 \text{ nm}$$

and $= .34.4\%$ at 580 nm

when $D = .84\text{cm}$

$$N_1 = 1 \times 10^{17} \text{ cm}^{-3}$$

$$\sigma_a(560) = .4 \times 10^{-16} \text{ cm}^2$$

$$\sigma_a(580) = .05 \times 10^{-16} \text{cm}^2$$

The amount lost to reabsorption is closer to 75% of these values because of the output coupling but reabsorption is still very large. The gain is thus very much smaller at 560 and 580nm than at 590nm and thus 590nm easily dominates. At 580, where reabsorption losses are smaller and the cross section for emission is larger, locking almost occurs but

is still not attained. At 560nm, locking does not even begin to take place.

A second, related result is that where there is reabsorption and strong injection, the spontaneous modes build quickly. Figure IV-11 shows what happens when the pump is delayed too long and the injection is strong under conditions of strong reabsorption. The spontaneous modes are strongly pumped and actually begin to lase befor the pumping pulse begins.

The third result is that for 600 and 620nm, where reabsorption does not occur for the singlet states, locking is complete during the pump pulse. In Figs IV-9 and 10, it can be seen that the spontaneous modes are five orders of magnitude less intense than the injected wavelengths at the peak of the pump pulse. Only when the pump has substantially fallen off and long after the injected pulse has ended, does the spontaneous modes begin to compete with the injected mode. At 620nm, the efficiency of the amplifier is 39% for much of the pulse. At 600 nm, the efficiency is 38.5%.

The fourth result is that the triplet state density remains small compared to the density of the upper laser level for much of the pump duration. The average time required for the triplet population to build up to one-fifth the population density of the upper laser level after pumping begins is 10.5ns. Furthermore, where the delay was 7 or 9ns, the triplet buildup was faster when singlet reabsorption is appreciable. This is because the upper laser level remaines at a fairly high density due the the injection and intersystem crossing takes place and thus N_5 builds quickly after the pumping starts.

According to equation II-2, the locking range range should grow larger for a smaller cavity Q. To test this, an additional computer run is made for 580nm with a delay time of 5ns and a mirror reflectivity of 20%. The result is shown in Figure IV-12. Injection locking still does not take place, but the output at the desired wavelength is much larger than when the mirror reflectivity is 95%. The explanation for this is that the cavity decay time is now much smaller and the effect of reabsorption is also smaller. The spontaneous modes now require more time to build up since their gain is now much smaller. The injected wavelength is now allowed to build up somewhat.

The way the spontaneous modes are included in the model derived in this paper may be somewhat incorrect. The buildup of those modes is strongly dependant upon the gain at each wavelength. The effects of that gain in these calculations may not be accurately taken into account because of the averaging process used to obtain the cross sections used. A more correct treatment is to divide the spectrum from 550 to 650nm into sections a nanometer wide or smaller and use the average cross sections times the width of the sections for the spontaneous modes. The effect would be to introduce mode competition between the spontaneous modes and produce a more realistic output.

The possible effects of the averaging process on the gain of the spontaneous modes is partially offset by allowing all the intensity of the spontaneous modes to go into just one

line. The intensity of a mode is directly porportional to the intensity of that mode before passing through the active region for constant gain. By allowing all of the energy to go into one mode, the effect of that mode on locking is far stronger than the individual modes that would realistically oscillate in the cavity. Taking many spontaneous modes into account will change the results of the work done here, but the work done here is still qualitatively useful.

V Summary, Conclusions, and Recommendations

The purpose of this chapter is to summarize the work done in this paper, give the conclusions reached, and then to give recommendations for additional work on the subject of injection locking.

Summary

A general set of rate equations to describe a dye laser is derived, using appropriate simplifications. The set of rate equations is supported by previous work. Comparison with work by Marowsky shows differences of less than 2%. Comparison with Lin's work shows good qualitative agreement for pulsed systems with pumping rates between 20 and 300 times the threshold pumping rate.

The rate equations are then extended to include injection locking. The extended rate equations show qualitative agreement with work by Ganeil *et al*. Their work could not be duplicated because of problems in obtaining some of the data they used.

The model developed is then used to compute results for cases of varying wavelengths and delay times between the injection and pump pulses. The results which may not be totally accurate, are still qualitatively useful and provide help in understanding injection locking.

Conclusions

The effects of reabsorption are critical in obtaining and maintaining locking. For wavelengths where reabsorption at the injected wavelength is large, injection locking does not occur. If reabsorption is small, injection locking is hard to achieve.

Spontaneous modes build up appreciably before the pump is started when the delay time is long, injection is strong, and reabsorption is large. When these conditions occur, the delay time must be kept short.

The population of the triplet state is kept small for most of the pump duration and therefore does not affect the performance of the laser to any great extent. One result of the analysis is that large reabsorption leads to a faster buildup of the triplet population. This is because the required threshold inversion is larger and leads to more intersystem crossing.

Low mirror reflectivities aid in injection locking. This is caused by increasing the time required for buildup in the injected modes and forcing the gain required for the injected mode to be larger than under conditions of higher mirror reflectivity.

Recommendations

The rate equations for injection locking derived here may not be accurate. The effects of competition between the cavity modes is not included. For following work, the model should be extended to include mode competition between these spontaneous modes.

A more accurate integration method should be used to obtain better results.

The model derived here should be compared to experimental results obtained form the amplifier at the Avionics Lab at Wright-Patterson AFB. The Amplifier at that facility will be ready for use at the end of 1978.

Further analysis using the model used here should be done on the amplifier. Many parameters can be varied and work should be done to find the most efficient way to obtain and maintain locking.

While not perfect, this paper is still useful in understanding injection locking and provides a basis for following work.

Bibliobraphy

1. Adler, R. "A study of locking phenomena in oscillators," Proceedings of the IRE, 34:351-357 (June 1946).

2. Bjorkholm, J. E. and H. G. Danielmayer, "Frequency control of a pulsed optical parametric oscillator by radiation injection," Applies Physics Letters, 15: 171-173 (Sept 1969).

3. Buczek, D. J. and R. J. Freiberg, "Hybrid injection locking of high power CO_2 lasers," IEEE Journal of Quantum Electronics, QE-8: 641-50 (July 1972).

4. Erickson, L. E. and Szabo, "Spectral narrowing of dye laser output by injection of monochromatic raditation into the laser cavity," Applied Physics Letters, 18: 433-5 (May 1971).

5. Ganiel, U., A. Hardy, and D. Treves, "Analysis of injection locking in pulsed dye laser systems," IEEE Journal of Quantum Electronics, QE-12 (11): 704-16 (Nov 1976).

6. Juramy, P., P. Flamant, and Y. Meyer, "Spectral properties of pulsed dye lasers," IEEE Journal of Quantum Electronics, QE-13 (10): 855-65 (Oct 1977).

7. Lin, C. "Studies of relaxation oscillations in organic dye lasers," IEEE Journal of Quantum Electronics, QE-11 (8): 602-9 (Aug 1975).

8. Maeda, M., T. Okada, O. Uchino, and Y. Miyazoe. "Spectral narrowing of a pulsed dye laser injected with monochromatic radiation," Japanese Journal of Applied Physics, 15 (9): 1731-6 (Sept 1976).

9. Marowsky, G. "A single-mode dye ring laser with output coupler using frustrated total internal reflection," Z. Naturforsch, 29a: 536-8 (1974).

10. Marowsky, G. "Principles of dye laser operation and dye laser tuning methods," Optica Acta, 23(11): 855-72 (Nov 1976).

11. Pease, A. A., O. G. Peterson, M. L. Spaeth, and W. M. Pearson. "An injection locked ring amplifier," Journal of Quantum Electronics, QE-13(9): 28-29 (Sept 1977).

12. Sahar, E. and D. Treves. "Excited singlet-state absorption in dyes and their effect on dye lasers," IEEE Journal of Quantum Electronics, QE-13(12): 962-7 (Dec 1977).

13. Snavely, B. "Flashlamp-excited organic dye lasers," Proceedings of the IEEE, 57(8): 1374-1389 (August 1969).

14. Sorokin, P. P. and J. R. Lankard, "Stimulated emission observed from an organic dye, chloroaluminum phtalocyanine," IBM Journal of Research Development, 10: 162-3 (March 1966).

15. Stover, H. L. and W. H. Steir, "Locking of laser oscillators by light injection," Applied Physics Letters, 8: 91-3 (Feb 1966).

16. Tang, C. L. and H. Statz. "Phase-locking of laser oscillators by injected signal," Journal of Applied Physics, 38(1): 323-4 (Jan 1967).

17. Turner, J. J., E. I. Moses, and C. L. Tang. "Spectral narrowing and electro-optical tuning of a pulsed dye laser by injection-locking to a cw laser," Applied Physics Letters, 27(8): 441-3 (Oct 1975).

18. Vrehen, Q. H. F. and A. J. Breimer. "Spectral properties of a pulsed dye laser with monochromatic injection," Optics Communications, 4(6): 416-20 (Feb 1972).

19. Johnson, T. H., P. L. Palumbo, and A. M. Hunter. "Kinetic simulation of high energy gas lasers," To be published in the Journal of Computational Physics.

Appendix A

The method of integration used to evaluate the coupled set of rate equations is a first-order Taylor expansion of the equations with flux limits. Flux limits means that certain rates of change are evaluated to determine the time step over which the equations are integrated. Under conditions which approach steady state, the steps are long. Under conditions of rapid change the time steps are smaller and get smaller as the changes get larger.

There are three ways to determine the integrator time step. The first is the time step fed into the program so that it is possible to fix the total length of time the equations are evaluated for. The second possibility is calculated by the program. The program looks at the ratio of the population density to the rate of change of that density and if it is smaller than the time step fed in, then the ratio is used as the time step. The third method of determining the time step is to multiply the previous dN/dt by the previous time step and then divide by the difference between the old and the new dN/dt. Basically, this is looking at how much the density has changed divided by the second derivative so that a check is made on the second order change in the populations. If this second ratio is smaller than the time step fed in or the first ratio evaluated, then the second ratio is used for the time step.

On the following page is a copy of the integrator used (Ref 19). SP(M) is the density of state M, DSDT(M) is the

dN/dt for state M, and DELT is the time step fed into the program.

```
      DIMENSION DTS(40),DELCHS(40),DDCHS(40)
      DATA FRAC1,FRAC2,CYCMAX/0.1,1.0,5000./
      CYCLIM=0.0
      TIME=0.
      ODOT=0.
      MT=1/NN
      DO 60 M=2,40
      OSP(M)=0.
      ODSDT(M)=0.
   60 DELSP(M)=SP(M)
      ADJ=10.
START OF PRIMARY CYCLE
   80 DT=DELT-TIME
      CALL DSPDT
      DO 100 M=2,40
      DDCH=0.
      DELCH=ABS((FRAC1*SP(M)+100.)/(DSDT(M)+1.E-100))
      IF(DELCH*FRAC2.GE.(DELT-TIME)) GO TO 100
      DSPDOT=ODSDT(M)-DSDT(M)
      DDCH=ABS((DELSP(M)+1.E-90)/(DSPDOT+1.E-100))
      DT=AMIN1(DDCH,DELCH,DT)
      DTS(M)=DT
      DELCHS(M)=DELCH
      DDCHS(M)=DDCH
  100 CONTINUE
      DO 101 M=2,40.
      OSP(M)=SP(M)
      ODSDT(M)=DSDT(M)
      DELSP(M)=DSDT(M)*DT
      SP(M)=SP(M)+DELSP(M)
      IF(SP(M).LT.0.) GO TO 200
      GO TO 101
  200 SP(M)=0.
  101 CONTINUE
      MT=0
      TIME=TIME+DT
      ADJ=10.
      CYCLIM=CYCLIM+1.
      IF(CYCLIM.LT.CYCMAX) GO TO 104
      STOP 222
  104 IF(TIME.LT.DELT)GO TO 80
      RETURN
      END
```

Appendix B

The plots in this section are results of calculations made to provide support for the model derived in this paper. The calculations are made for comparixon with work by Gerd Marowsky (Chapter 4). Figures B-1a, b, and 2a are made at 560, 590, and 620nm respectively under constant pump and including reabsorption. They show that as soon as lasing begins, triplet reabsorption begins to decrease the output of the laser. The plots also show that reaching steady state takes a relatively long time and that figure B-2a is still just attaining steady state after 2.5×10^{-7} sec. The difference between the results here and Marowsky's predicted results is 2% and if the calculations are carried out far enough this difference will grow smaller since the output of the calculated result is still dropping slightly.

In figures B-2a, 3a, and 3b the plots are at wavelengths of 560, 590, and 620nm respectively and under a constant pump. The difference between these and the first three is that reabsorption is neglected. As can be seen, the output reaches a steady state value very quickly. These steady state values are only .5% different from the ones predicted by Marowsky's equation for efficiency (Eq IV-1).

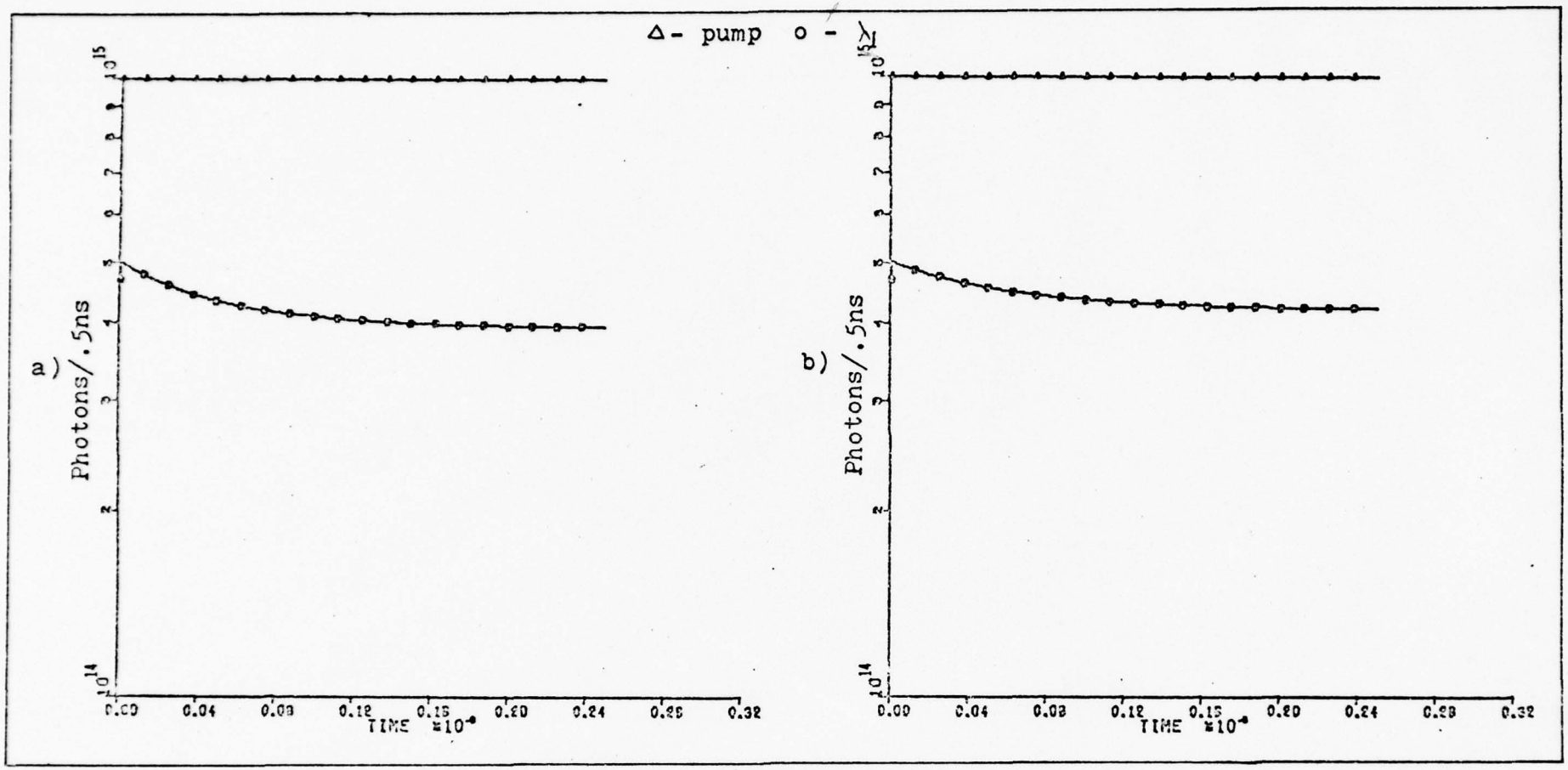

Figure B-1: Results of computations for obtaining steady state conditions.

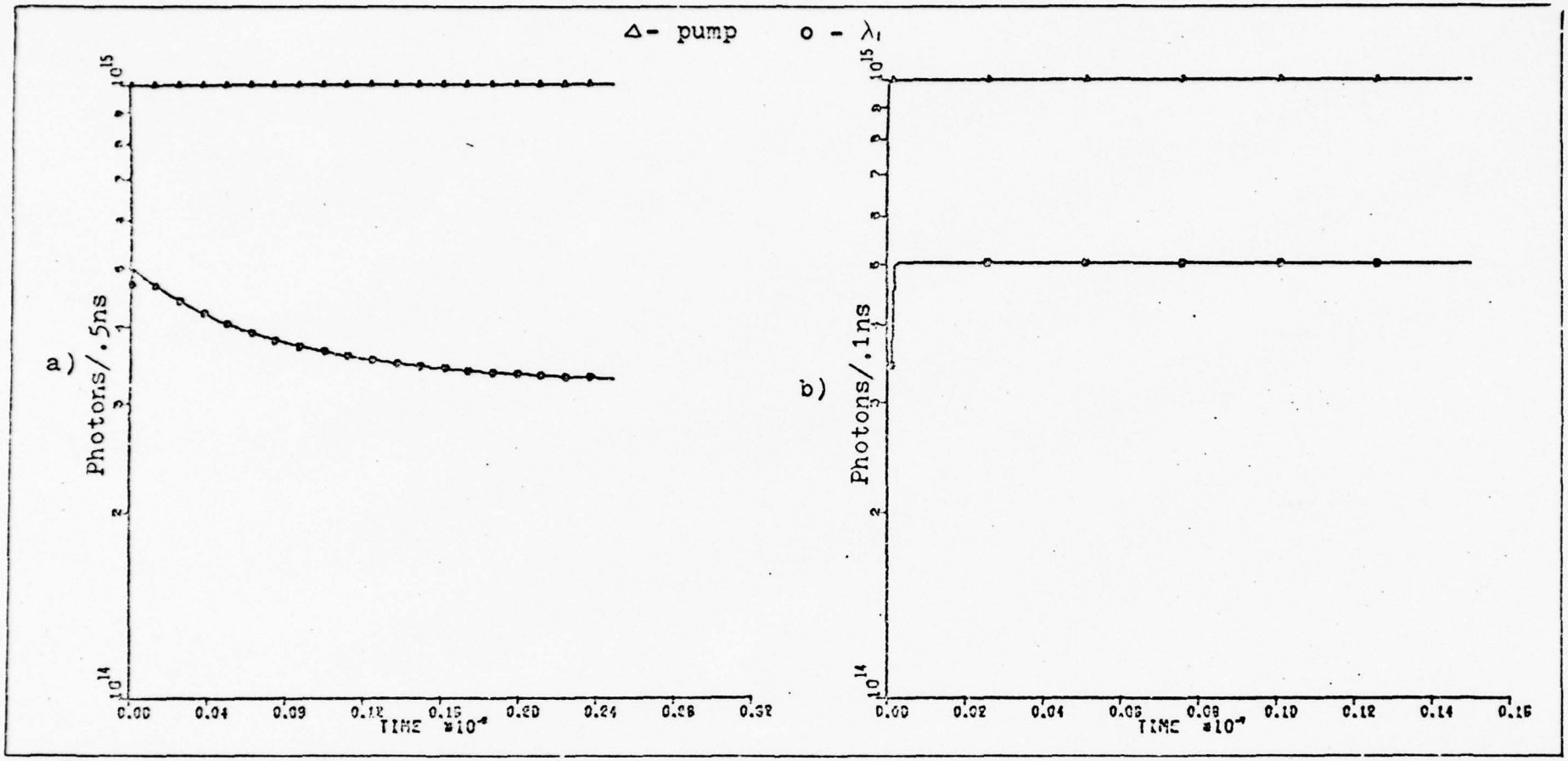

Figure 3-2: Results of computations for obtaining steady state conditions.

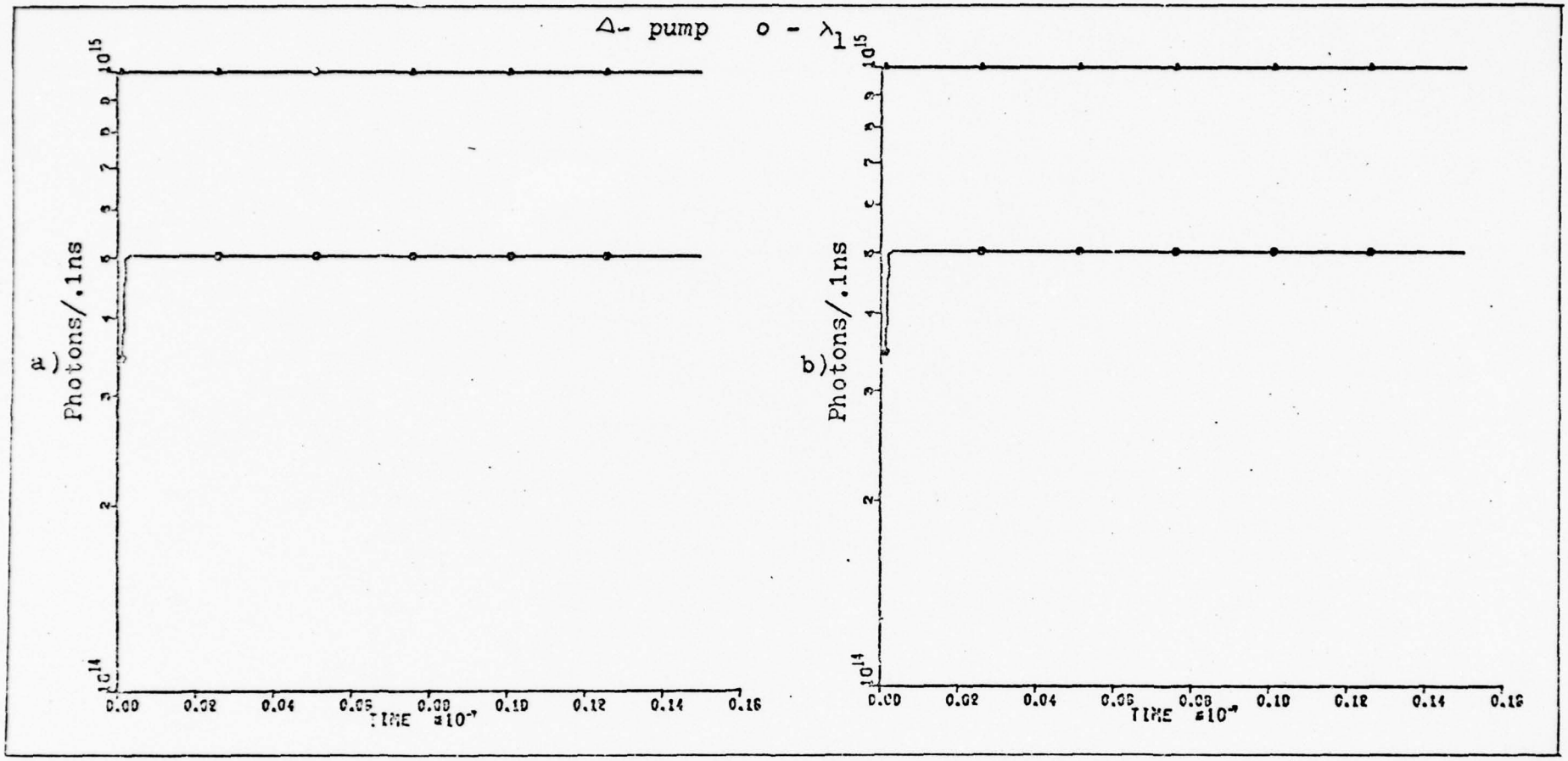

Figure B-3: Results of computations for obtaining steady state conditions.

Appendix C

The plots in this section are the results of calculations made from the model derived in this paper and are used for comparison with work by Lin. The plots presented here show good qualitative agreement to the work by Lin. Lin's results are shown in figure IV-1. The plots presented here are for a cavity with a decay time of 50 ps. The dye has an upper laser level decay time of 2 ns. The threshold pump rate is 1.5×10^{25} sec^{-1} (Eq IV-2). The plots are made for pump rates above threshold as indicated.

From the plots it can be seen that the decay of the spikes is gaussian. For increasing pump rates, the duration of the spikes decrease. In addition, as the pump gets further above threshold, lasing begins sooner and the output begins to closely resemble the shape of the pump pulse. All of these results are consistent with the work done by Lin.

Figures 4 and 5 are semi-log plots of the results for the pump rates above threshold given. These figures show the exponential damping of the spikes.

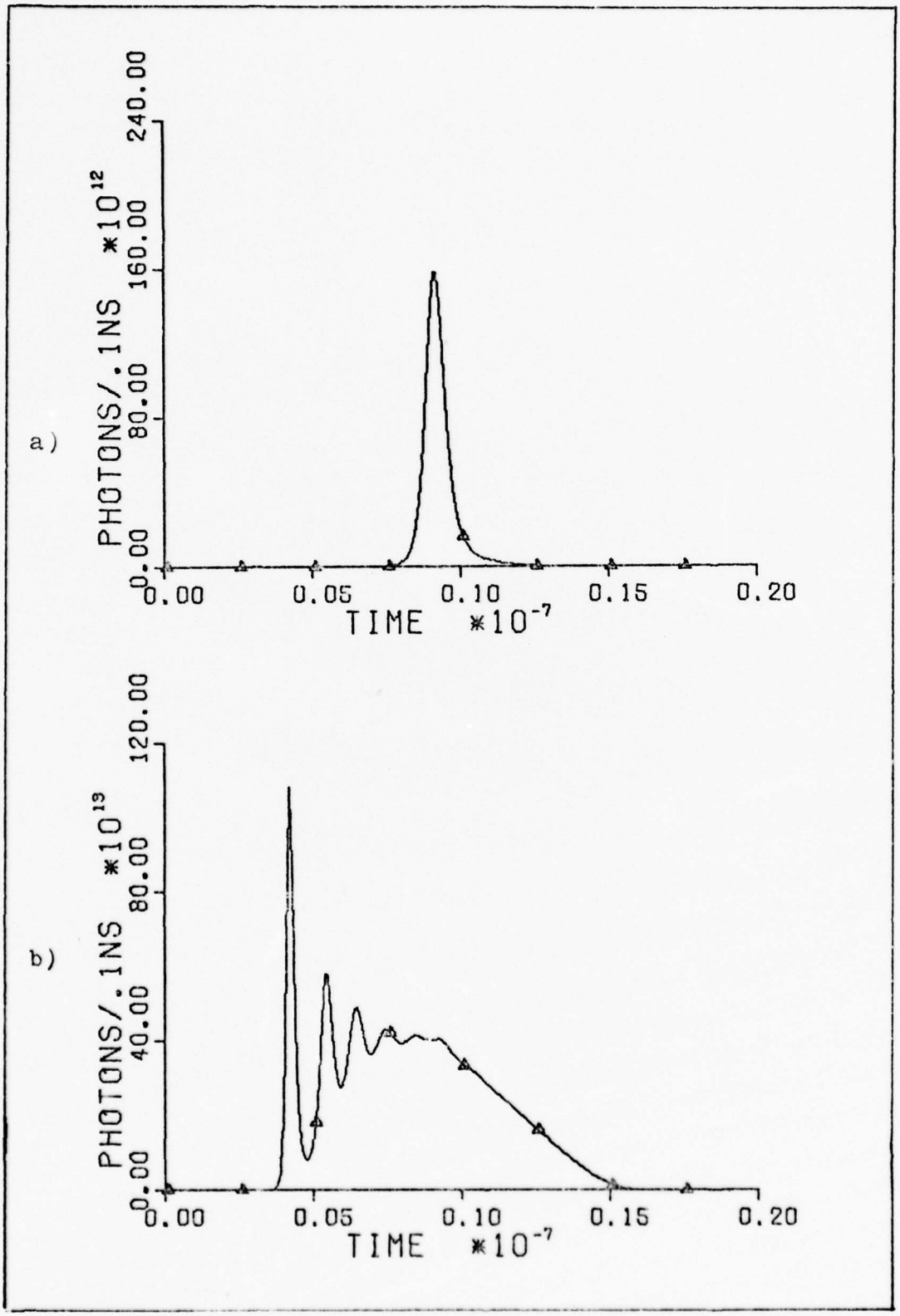

Figure B-1: Plots of the solutions of the rate equations. Figure (a) is for 14 times the threshold pump rate and (b) is for 50 times threshold.

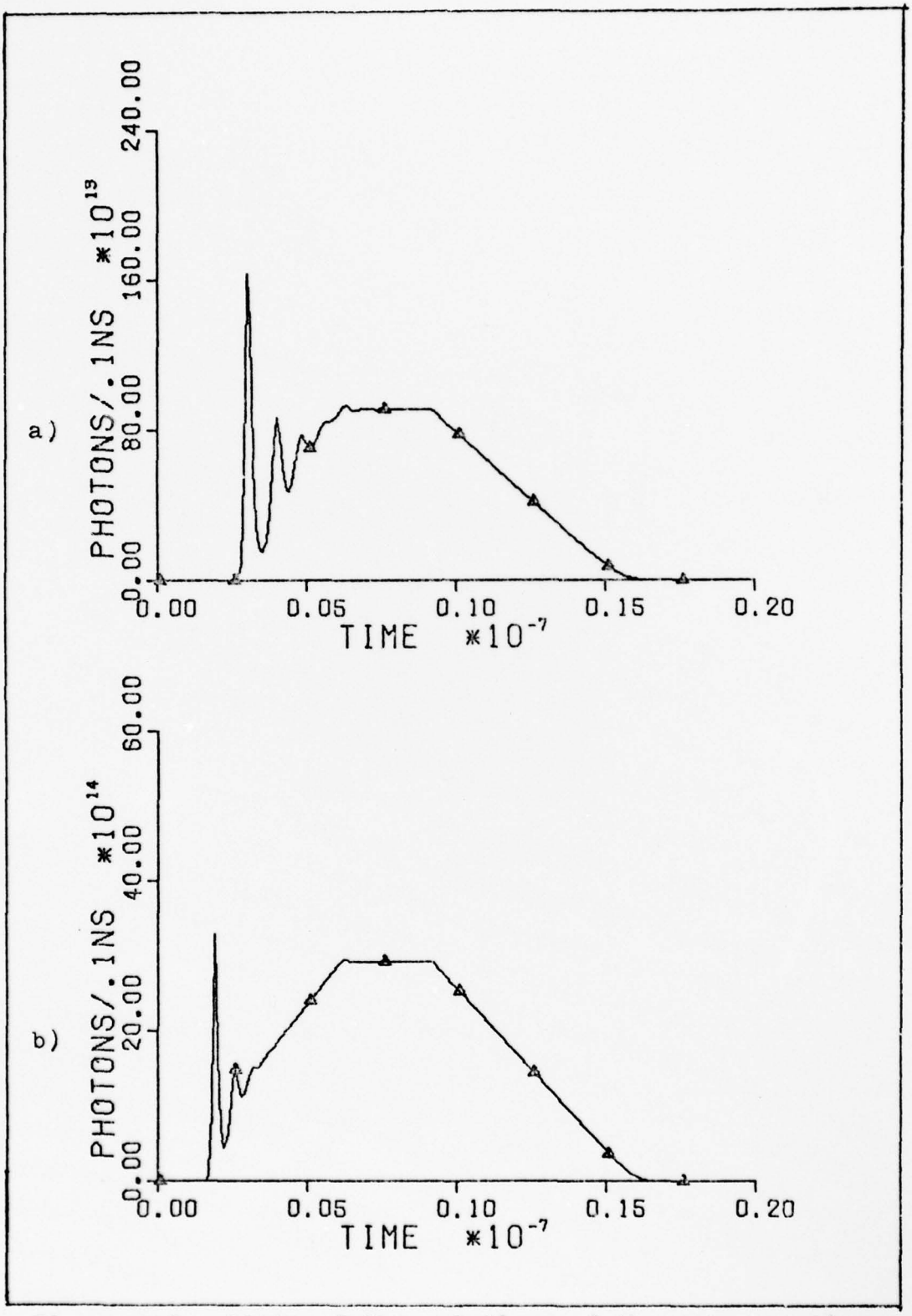

Figure B-2: Plots of the solutions of the rate equations. Figure (a) is for 100 times the threshold pump rate and (b) is for 300 times threshold.

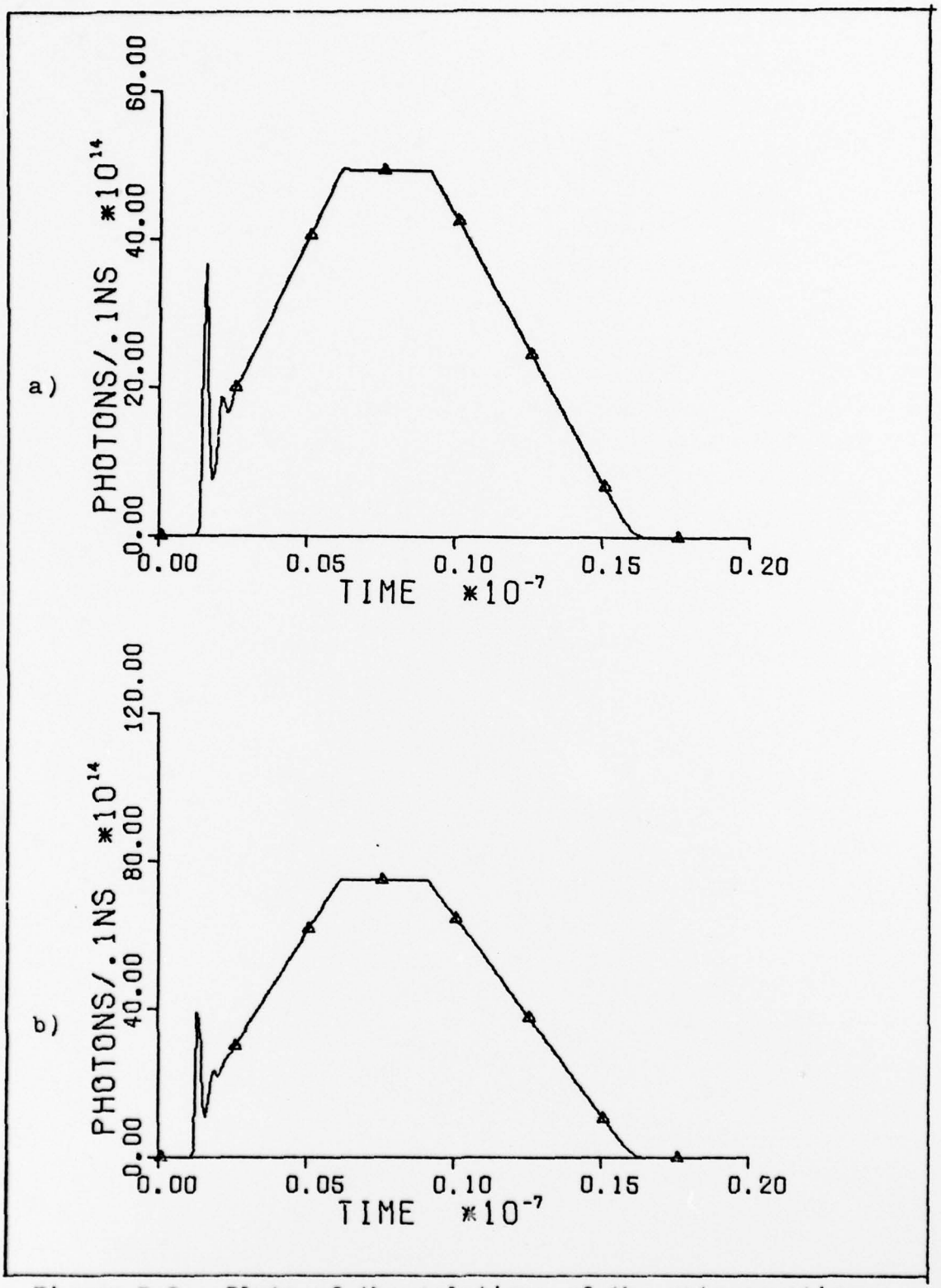

Figure B-3: Plots of the solutions of the rate equations. Figure (a) is for 500 times the threshold pump rate and (b) is for 750 times threshold.

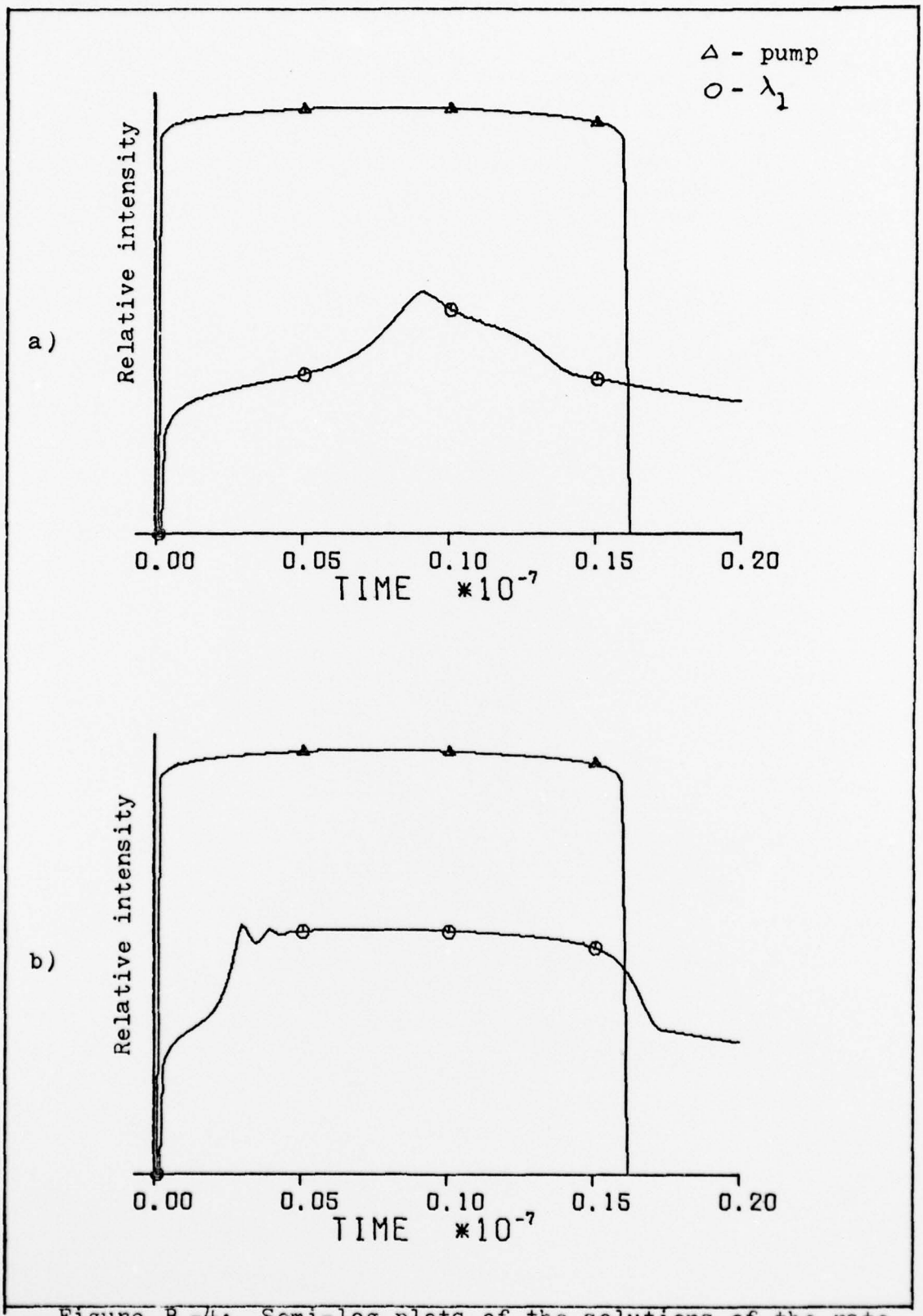

Figure B -4: Semi-log plots of the solutions of the rate equations. Figure (a) is for 14 times the threshold pump rate and (b) is for 100 times threshold.

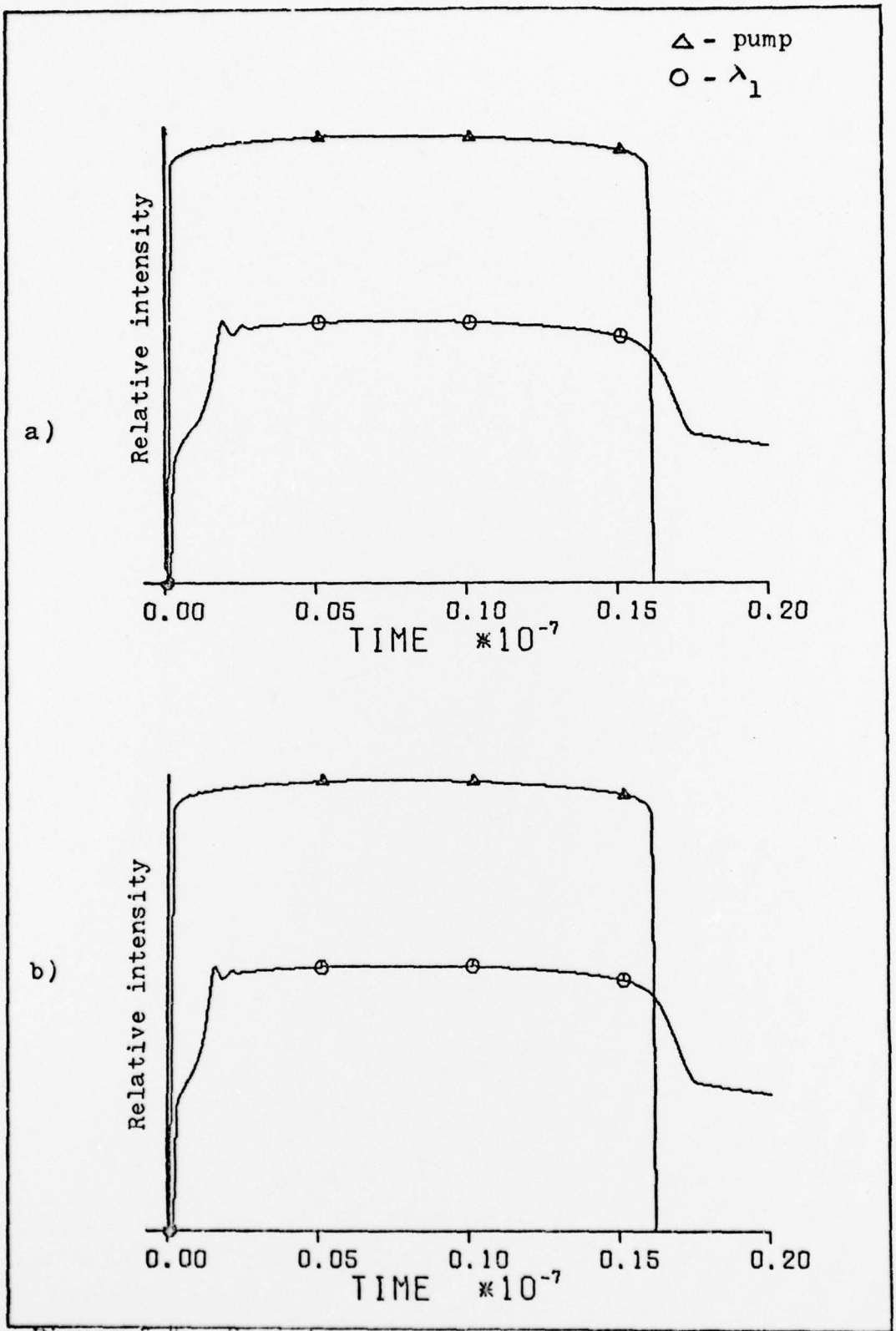

Figure 5-4: Semi-log plots of the solutions of the rate equations. Figure (a) is for 300 times the threshold pump and (b) is for 500 times threshold.

Appendix D

In this section are the plots for injection locking obtained from the rate equation model derived in this paper. The plots are for injections at 560, 580, 600, and 620 nm. Delay times of 1, 3, 7, and 9 ns are used for all wavelengths except for 560 which is not done for 9 ns. Mirror reflectivity is 95% and the cross sections used are obtained from figure II-2.

From the plots, the effects of reabsorption are easily seen for 560 and 580 nm where locking is never really achieved. At 560, 600, and 620 nm, the effects of delay time can be seen. The most efficient delay time is between 3 and 7 ns. Locking is complete at 600 and 620 nm for all delay times and the spontaneous mode is due mainly to fluorescent decay which is assumed to go into that mode.

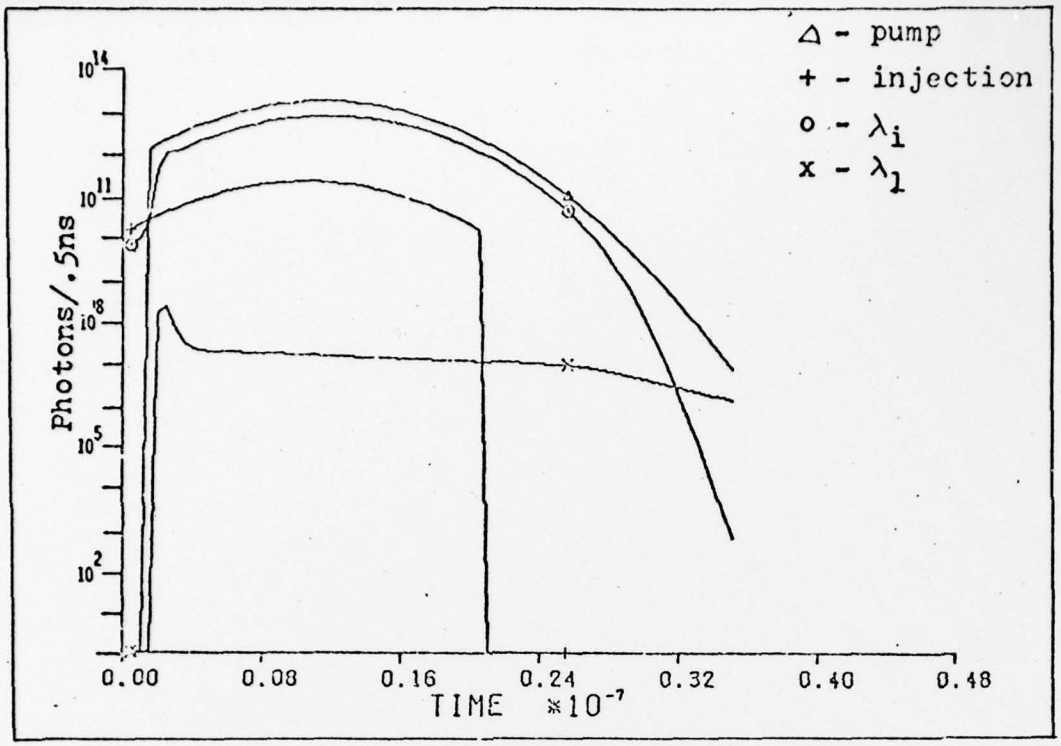

Figure D-1a: Result for computation of injection locking. Injection is at 620 nm and the delay time is 1 ns.

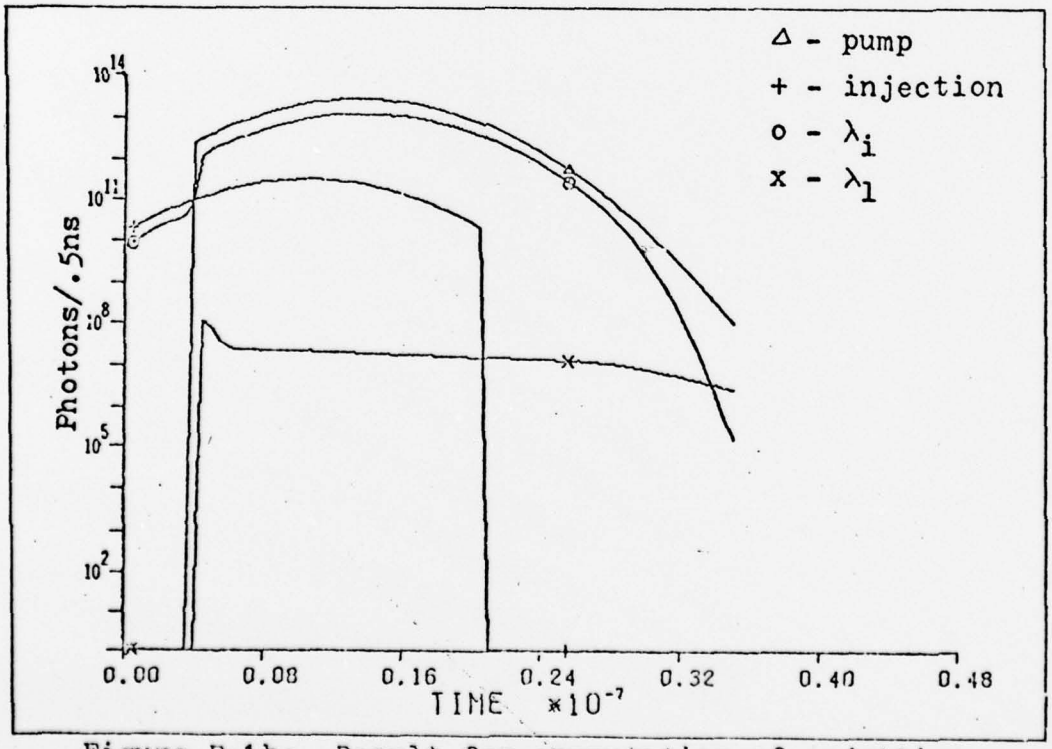

Figure D-1b: Result for computation of injection locking. Injection is at 620 nm and the delay time is 3 ns.

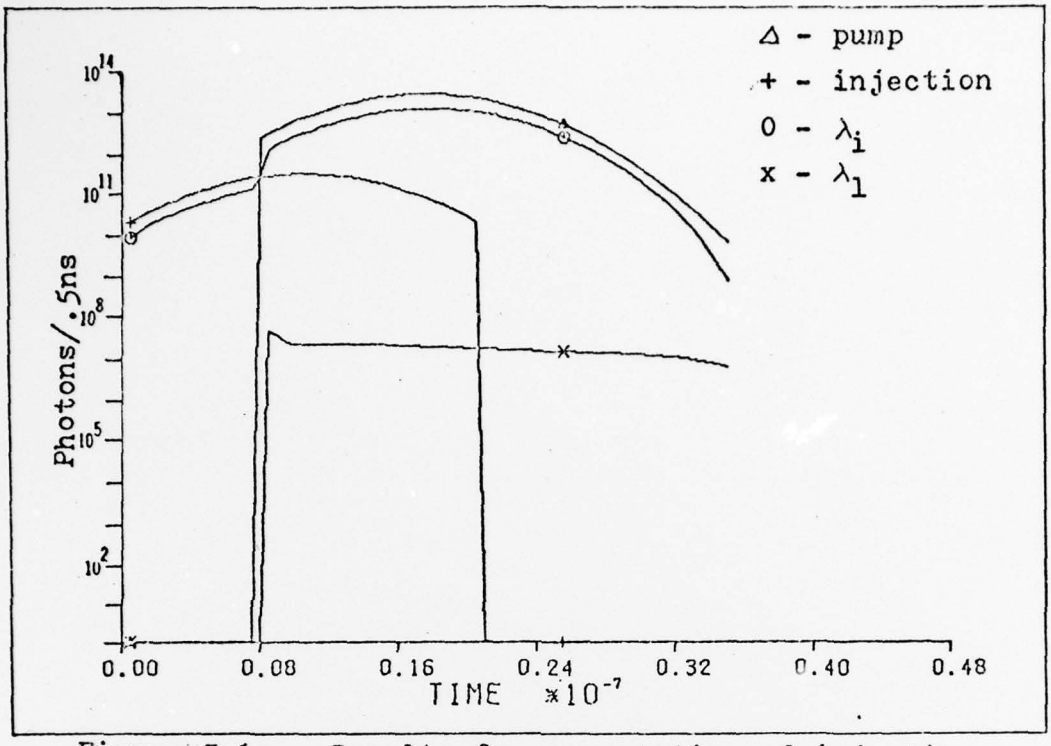

Figure D-1c: Results for computation of injection locking. Injection is at 620 nm and the delay time is 7 ns.

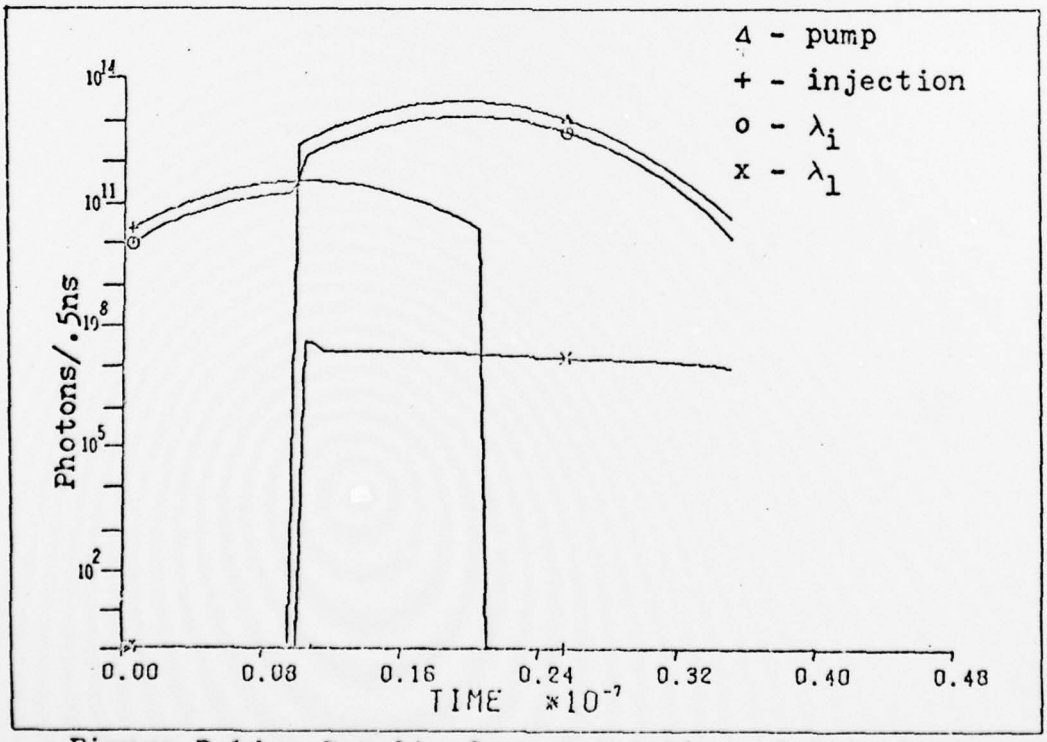

Figure D-1d: Results for computation of injection locking. Injection is at 620 nm and the delay time is 9 ns.

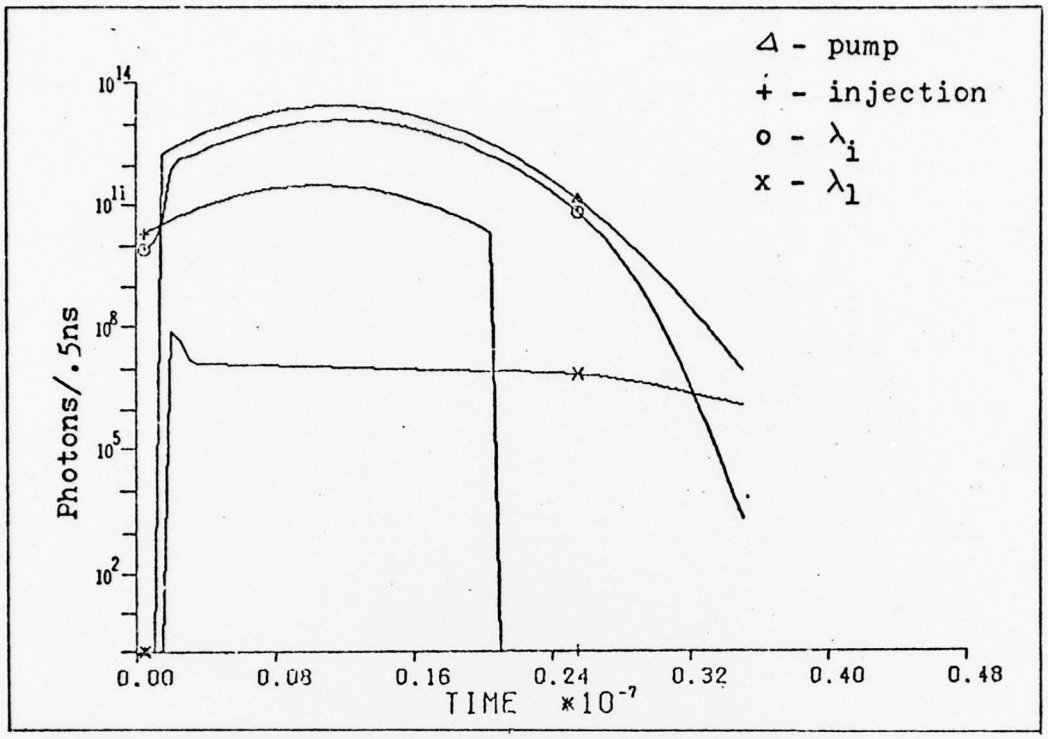

Figure D-2a: Result for computation of injection locking. Injection is at 600 nm and the delay time is 1 ns.

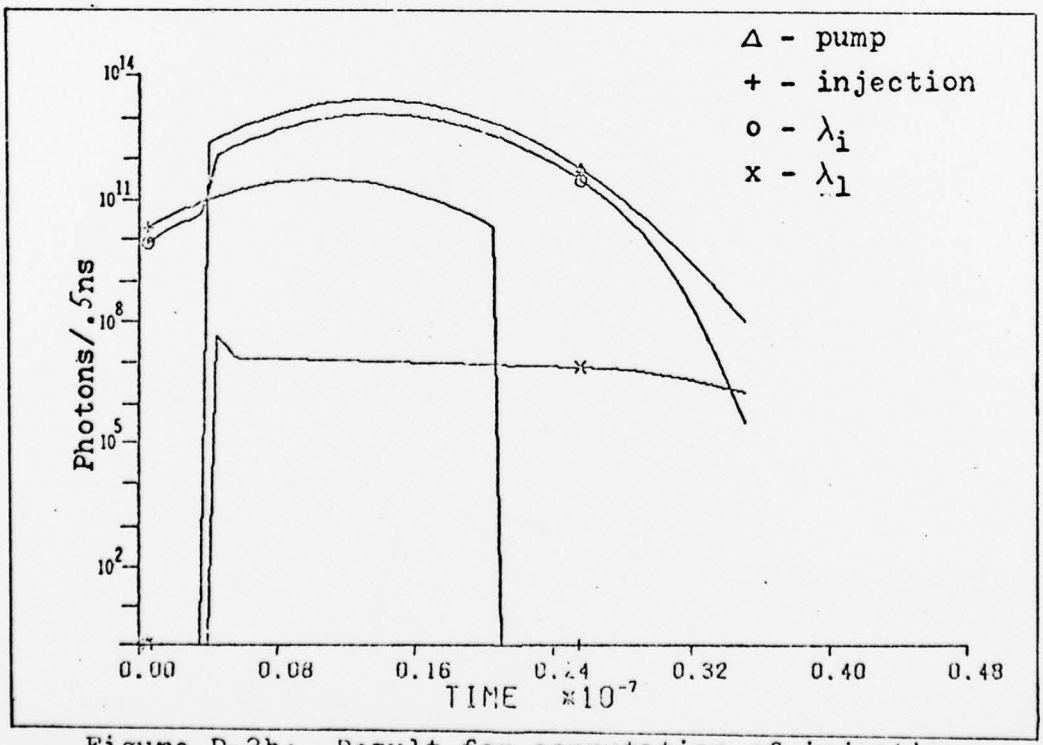

Figure D-2b: Result for computation of injection locking. Injection is at 600 nm and the delay time is 3 ns.

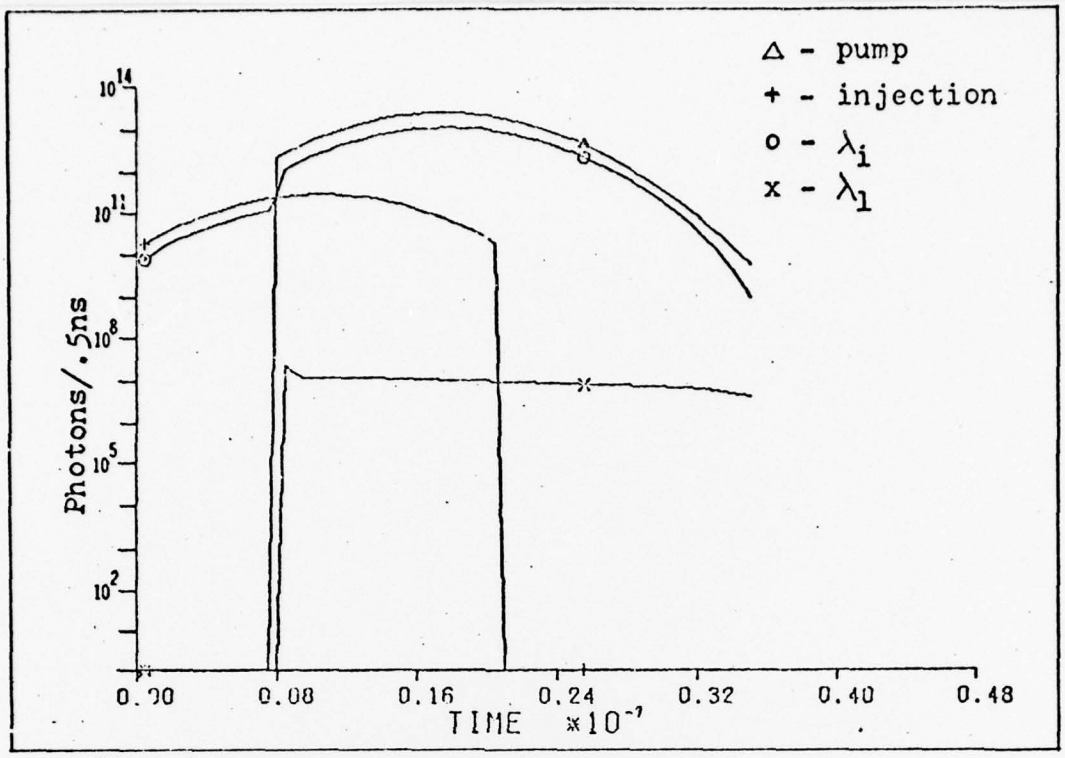

Figure D-2c: Result for computation of injection locking. Injection is at 600 nm and the delay time is 7 ns.

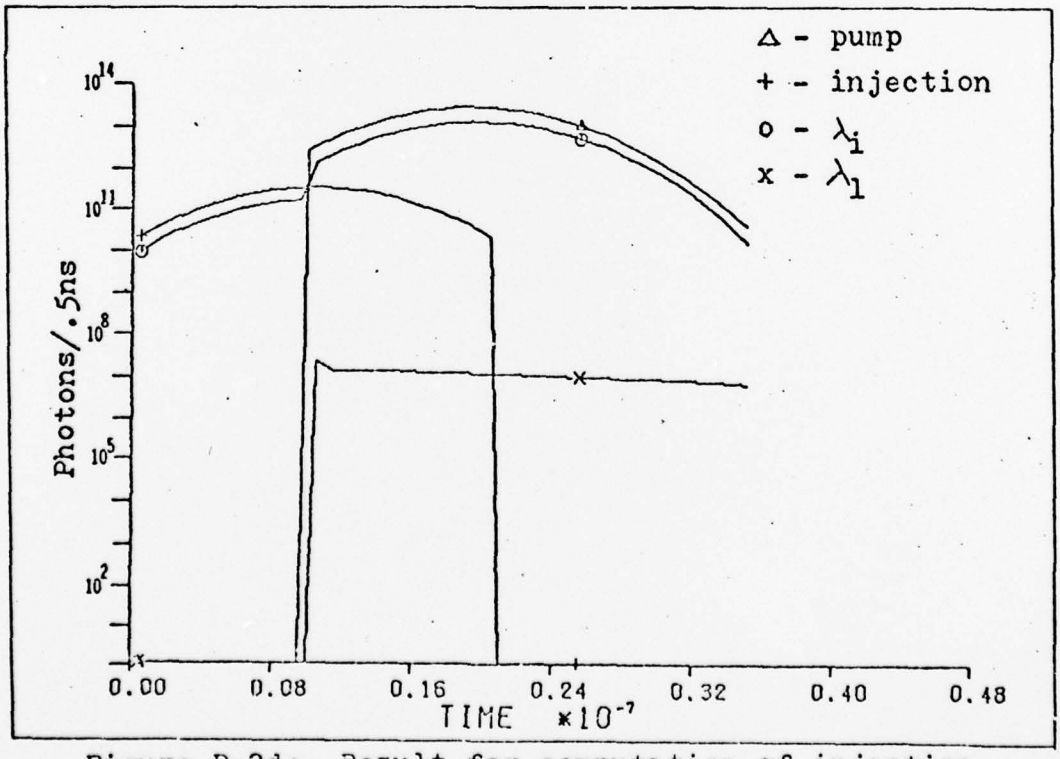

Figure D-2d: Result for computation of injection locking. Injection is at 600 nm and the delay time is 9 ns.

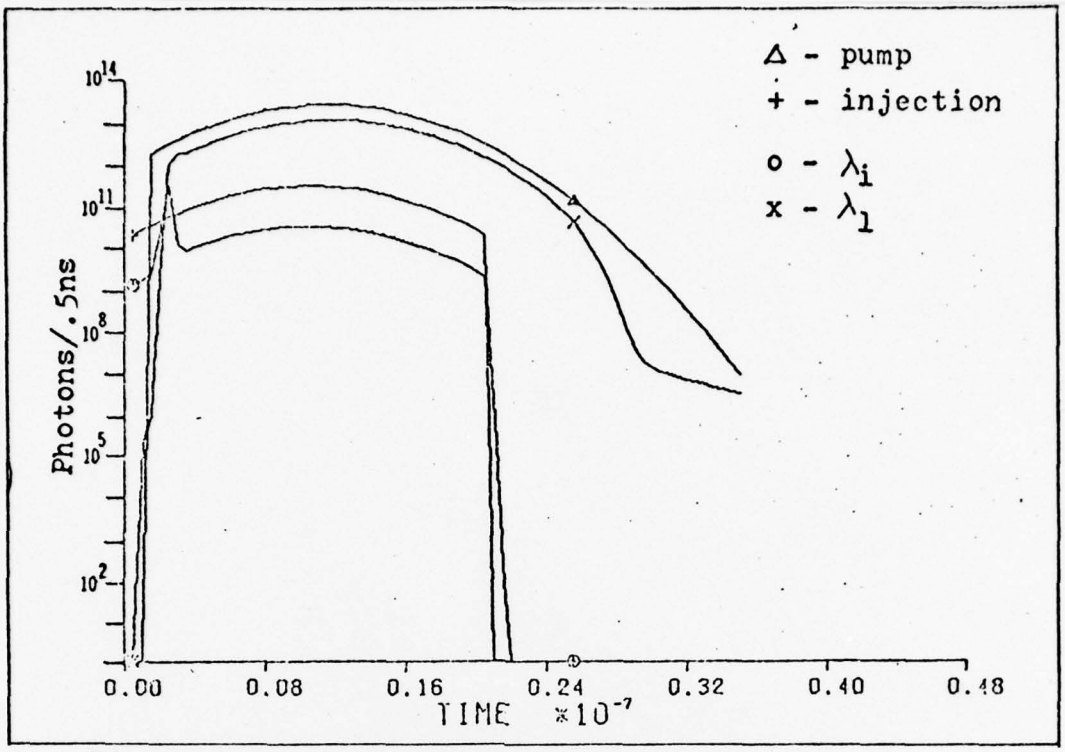

Figure D-3a: Result for computation of injection locking. Injection is at 580 nm and the delay time is 1 ns.

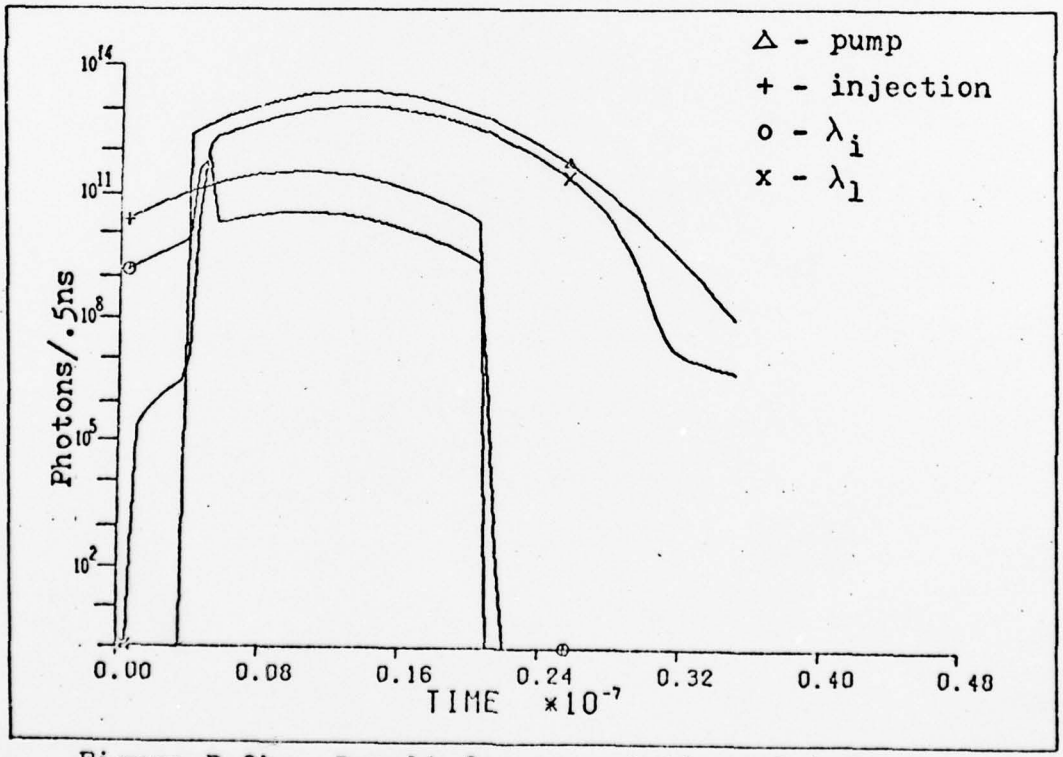

Figure D-3b: Result for computation of injection locking. Injection is at 580 nm and the delay time is 3 ns.

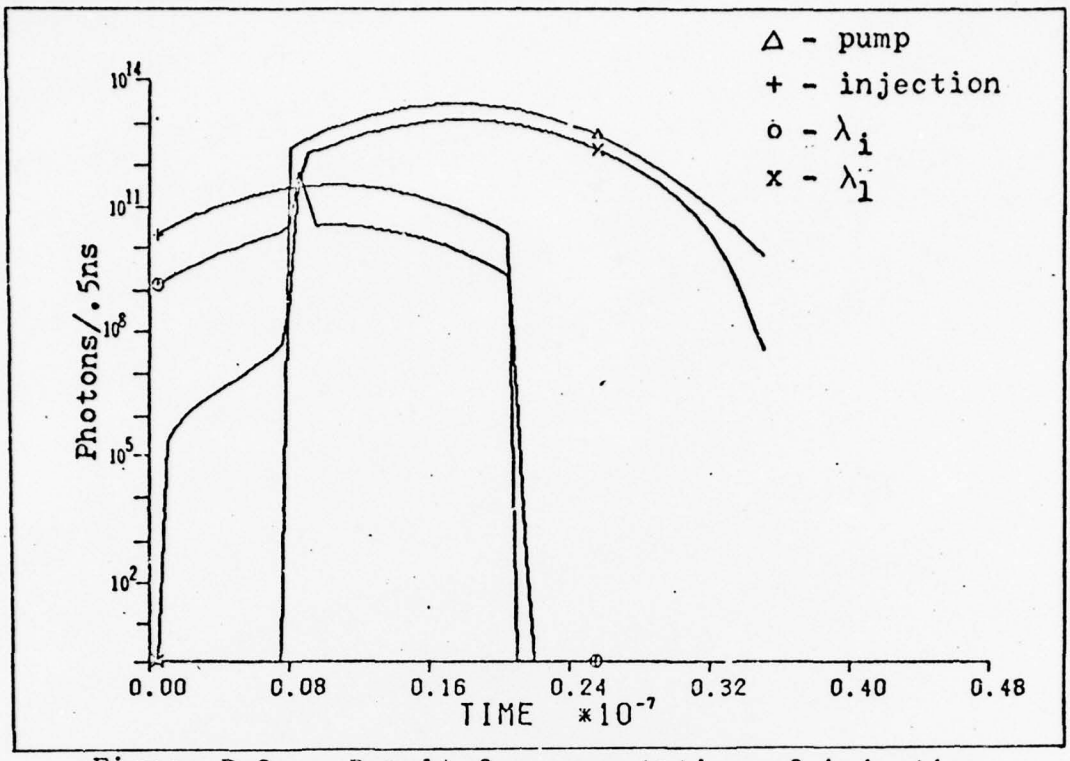

Figure D-3c: Result for computation of injection locking. Injection is at 580 nm and the delay time is 7 ns.

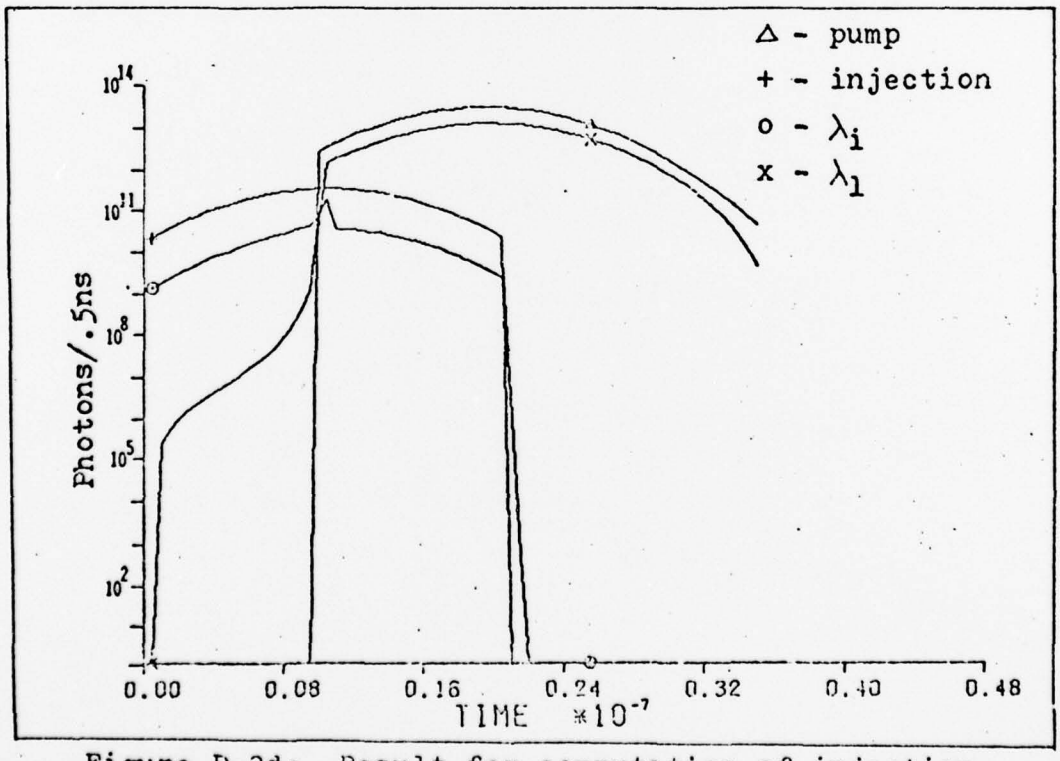

Figure D-3d: Result for computation of injection locking. Injection is at 580 nm and the delay time is 7 ns.

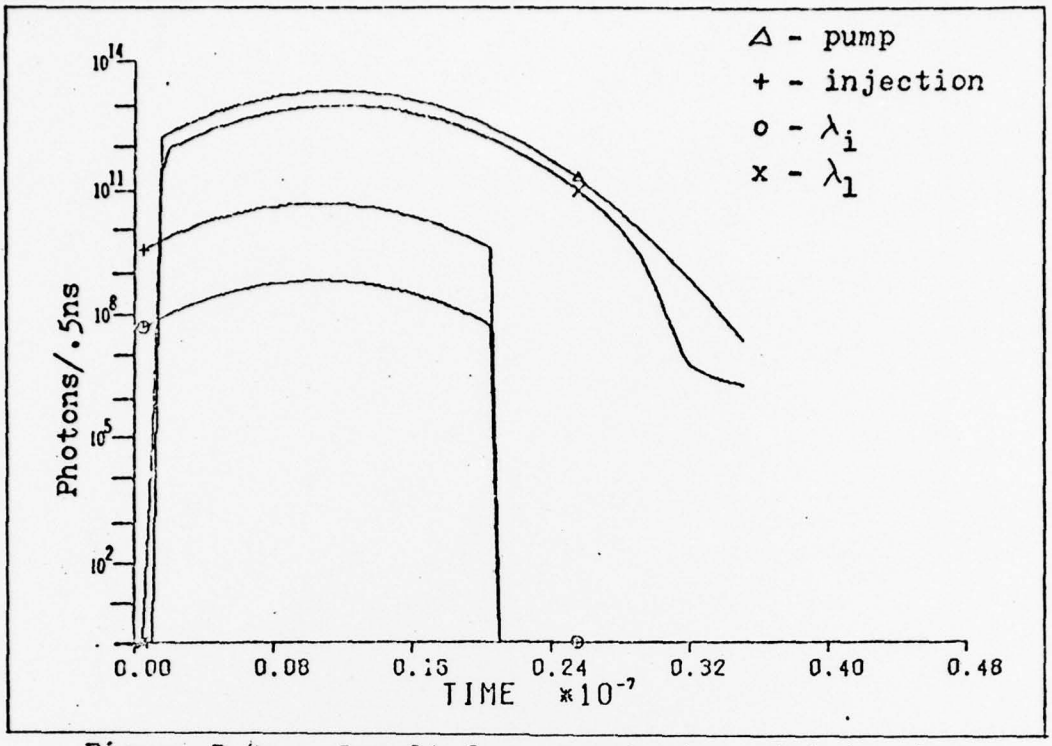

Figure D-4a; Result for computation of injection locking. Injection is at 560 nm and the delay time is 1 ns.

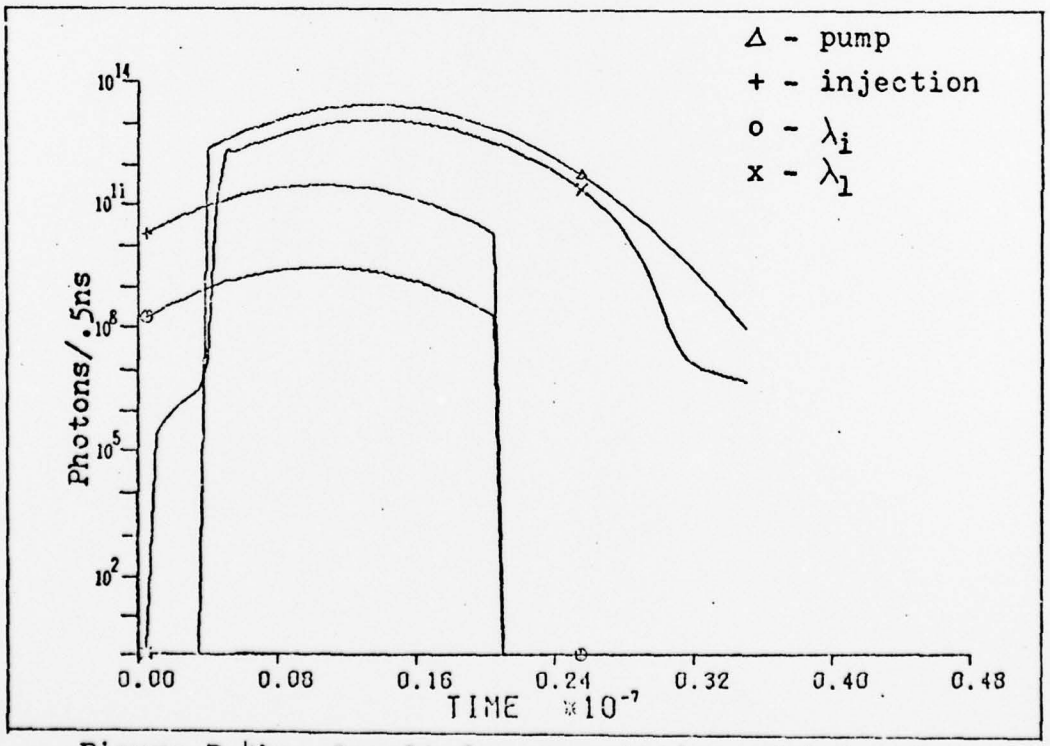

Figure D-4b: Result for computation of injecgion locking. Injection is at 560 nm and the delay time is 3 ns.

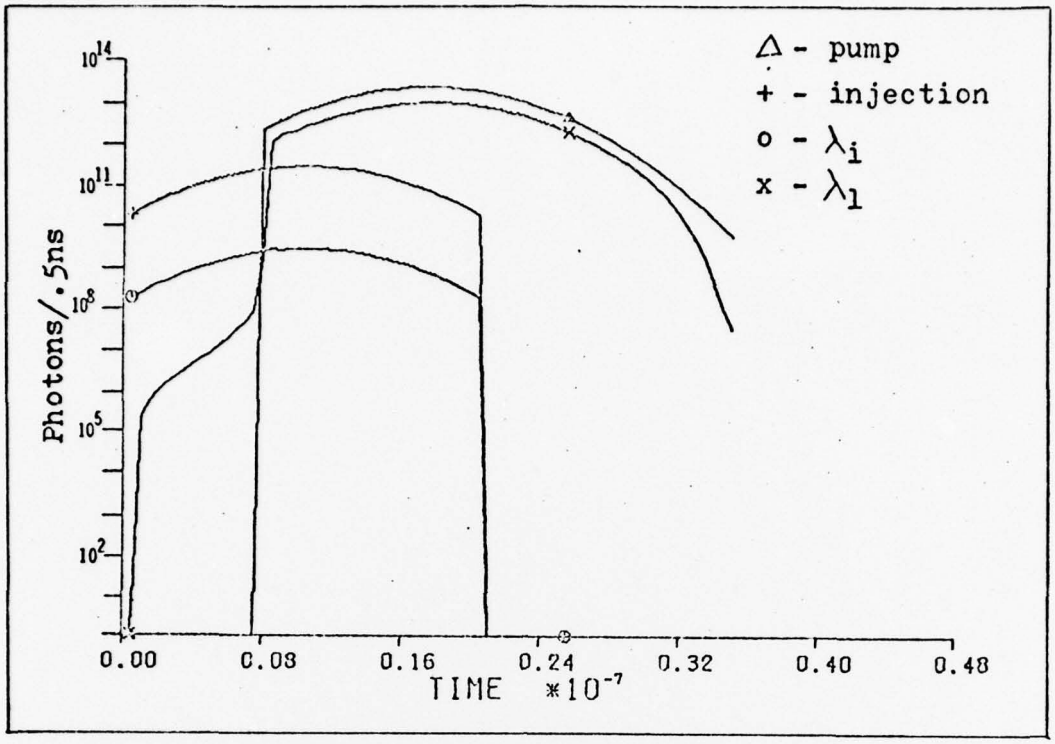

Figure D-4c: Result for computation of injection locking. Injection is at 560 nm and the delay time is 1 ns.

Unclassified
SECURITY CLASSIFICATION OF THIS PAGE (When Data Entered)

REPORT DOCUMENTATION PAGE		READ INSTRUCTIONS BEFORE COMPLETING FORM
1. REPORT NUMBER AFIT/GEP/PH/78D-15	2. GOVT ACCESSION NO.	3. RECIPIENT'S CATALOG NUMBER
4. TITLE (and Subtitle) Analysis of an Injection-locked Dye Ring Laser Amplifier		5. TYPE OF REPORT & PERIOD COVERED MS Thesis 6. PERFORMING ORG. REPORT NUMBER
7. AUTHOR(s) James C. Vetter		8. CONTRACT OR GRANT NUMBER(s)
9. PERFORMING ORGANIZATION NAME AND ADDRESS Air Force Institute of Technology (AFIT-EN) Wright-Patterson AFB, Ohio 45433		10. PROGRAM ELEMENT, PROJECT, TASK AREA & WORK UNIT NUMBERS
11. CONTROLLING OFFICE NAME AND ADDRESS Air Force Avionics Lab (AFAL) Wright-Patterson AFB, Ohio 45433		12. REPORT DATE October 1978 13. NUMBER OF PAGES 74
14. MONITORING AGENCY NAME & ADDRESS(if different from Controlling Office)		15. SECURITY CLASS. (of this report) Unclassified 15a. DECLASSIFICATION/DOWNGRADING SCHEDULE

16. DISTRIBUTION STATEMENT (of this Report)

Approved for public release; Distribution unlimited

17. DISTRIBUTION STATEMENT (of the abstract entered in Block 20, if different from Report)

18. SUPPLEMENTARY NOTES

Approved for public release; IAW AFR 190-17

JOSEPH P. HIPPS, MAJOR, USAF
Director of Information 1-23-79

19. KEY WORDS (Continue on reverse side if necessary and identify by block number)

Injection Locking
ring laser
laser amplifier

20. ABSTRACT (Continue on reverse side if necessary and identify by block number)

A rate equation model of an injection-locked dye ring laser amplifier is derived. The amplifier is a design by Pease *et al*. The model is compared to work by G. Marowsky, C. Lin, and U. Ganiel *et al* and is shown to compare well. The model is then used for analysis of the amplifier. The conditions of the amplifier that are varied are the injected wavelength, delay time between injection and pump pulses, and the mirror reflectivity. Results show that reabsorption of photons at

DD FORM 1 JAN 73 1473 EDITION OF 1 NOV 65 IS OBSOLETE

Unclassified
SECURITY CLASSIFICATION OF THIS PAGE (When Data Entered)

the injected wavelength by the dye has serious effects on locking and that varying the mirror reflectivity partially alleviates this situation. The best decay times were found to be between 3 and 7 ns.